

DEVELOPMENT AND EVALUATION OF NOVEL TRIAZOSPIROCYCLES AS HISTONE DEMETHYLASE
INHIBITORS

by

SHANE M. WALLS

B.A., University of Colorado, 2014

A thesis submitted to the
Faculty of the Graduate School of the
University of Colorado in partial fulfillment
of the requirement for the degree of
Master of Science
Department of Chemistry and Biochemistry

2017

This thesis entitled:
Development and Evaluation of Novel Triazospirocycles as Histone Demethylase Inhibitors
written by Shane M Walls
has been approved for the Department of Chemistry and Biochemistry

(Dr. Xiang Wang)

(Dr. Wei Zhang)

Date_____

The final copy of this thesis has been examined by the signatories, and we find that both the content and the form meet acceptable presentation standards of scholarly work in the above mentioned discipline.

ABSTRACT

Walls, Shane M. (M.S., Department of Chemistry and Biochemistry)

Development and Evaluation of Novel Triazospirocycles as Histone Demethylase Inhibitors

Thesis directed by Associate Professor Xiang Wang

Gene expression is guided by epigenetic regulation, which can turn genes on and off, allowing for varied cellular phenotypes. This is accomplished by adding or subtracting functional groups on the tails of proteins around which DNA coils. These changes are made by enzymes such as histone methyltransferases (HMTs) that add methyl groups to specific lysine residues found on histone tails or histone demethylases (HDMs) that remove them. The process of histone modification is necessary for cellular growth and differentiation, but irregular activity is associated with mental disabilities and diseases such as cancer. These ideas will be briefly discussed in a broad overview along with a review of the current state of research regarding histone lysine methylation and demethylation.

What follows is the discovery and enhancement of a JHDM1A inhibitor built on a novel triazospirocyclic scaffold. The lead compound, HTS12214, was discovered by high-throughput screening (HTS) of the Maybridge library and a structure-activity relationship study was then conducted with the aim of improving the binding affinity toward JHDM1A. A series of 24 analogs was synthesized and their binding affinities were evaluated using a fluorescence polarization based competition binding assay previously developed by the Wang Lab.

Dedicated to my brilliant daughter, Hailey, who constantly reminds me that I'll never be too old to laugh at a poop joke. When the stresses of life become overwhelming, you always know how to make me smile. You are such a bright young lady in both mind and manner. You inspired me to be a better person. You gave me the motivation to succeed. You are the coolest person I've ever met and I want to be just like you when I grow up.

ACKNOWLEDGEMENTS

To Prof. Xiang Wang, I would like to extend my sincerest gratitude for providing me the opportunity to conduct research in your lab. You have been a great mentor to me since I was an undergraduate back in my biochem days. You are friendly and approachable while maintaining honesty in your responses. Thank you for being flexible and understanding during my times of stress and indecisiveness.

I would also like to thank my lab mates Dr. Jessica Podoll, Dr. Patrick Barbour, Dr. Wei Wang, and (Future Dr.) Brendan Griffiths. Jessica, you were a fantastic mentor when I was but a wee little undergraduate learning how to maintain cell lines and purify proteins. Thank you for your careful teaching and patience when I asked the same questions roughly fourteen thousand times. Patrick, I really appreciate the time you took to explain techniques and chemistry in depth. Your explanations reminded me how all of the advanced, complicated concepts related back to the basics. This painted a clear picture for me and I learned a lot more from you than I let on. Wei, thank you for conducting all the biological assays and taking the time to thoroughly explain the results when I had questions. Brendan, thank you for your help with lab supplies and writing. I enjoyed our late-night exam grading conversations and chemistry-related emails with absurd and unrelated memes attached.

To my good friend and colleague, Tianyi Yang, I thank you so much for your friendship. From our first day of orientation, you have been cheerful, positive, and knowledgeable in all things organic. You were (and still are) always available for advice when I was having problems in the lab, the classroom, or personal matters. I admire your understanding of chemistry, which is vastly superior to my own (you can't argue with me this time because now it's written in a book).

A well-deserved shout out to my amazingly patient girlfriend, Lacey Turner. Thank you for listening to me as I babbled about my chemistry drivel like a bumbling fool. You let me talk crazy talk at you like a mad scientist to help me solve problems. You're always supportive, but you also know just the right time to deliver a verbal jab which never fails to make me laugh. Without you, I would have gone crazy years ago.

I am grateful to my supervisors, Dave Moreno and Andy Ren at Array BioPharma, not just for guiding me in honing my chemistry skills, but for being understanding and flexible with my graduate research schedule. I was able to use the things you taught me to expedite the synthesis and purification process while increasing yields. I greatly appreciate your mentorship.

I saved the best for last. Thank you to my parents, Dean and Lisa, because without them, I wouldn't be the person I am today. I wouldn't even be a person at all, actually. I would be a nothing (both literally and figuratively). Thank you both for your love and encouragement through all of life's obstacles, especially during the troubling times when things seemed hopeless. I'm lucky to have strong, hard-working parents that refused to let me give up.

CONTENTS

Chapter 1	Introduction	1
1.1	Epigenetics and the structure and function of Histone proteins.....	1
1.2	Histone Modifications	2
1.3	Histone Demethylases	3
1.4	Current state of HDM inhibitor research	6
Chapter 2	Structure-Activity Relationship Study.....	12
2.1	Discovery of a unique JHDM1A inhibitor	12
2.2	New spirocycle “hit” compound	13
2.3	Synthetic hurdles	16
2.4	Data and discussion	19
2.4.1	R ₁ -Substitutions.....	20
2.4.2	R ₂ -Substitutions.....	20
2.4.3	R ₃ -substitutions.....	22
2.4.4	Rhodanine methylene substitutions.....	23
2.5	Final analogs.....	24
2.6	Concluding remarks	26
Chapter 3	Experimental Section	28
Chapter 4	Characterization data.....	32
References	45

LIST OF TABLES

Table 2.1. Activity of inhibitors discovered in the Maybridge library	13
Table 2.2. R ₁ -R ₃ substitutions and observed binding constants in JHDM1A.....	19

LIST OF FIGURES

Figure 1.1. Histone arrangement within nucleosome.	1
Figure 1.2. Methylation states of lysine residues.	4
Figure 1.3. FAD-dependent oxidative demethylation mechanism occurring in HDMs that do not contain a Jumonji-C domain.	5
Figure 1.4. Binding and mechanism of JHDMS.....	5
Figure 1.5. HDM inhibitors in active clinical trials.....	7
Figure 1.6. Previously identified inhibitors of JHDMS.....	9
Figure 1.7. Methylstat and methylstat probes developed by the Wang lab.	10
Figure 2.1. Structures of JHDM1A inhibitors discovered from high-throughput screening of the Maybridge library.....	13
Figure 2.2. Sites of variation.	20
Figure 2.3. Analogs with methyl and unsubstituted rhodanine.	22
Figure 2.4. Aldol condensation of rhodanine derivatives.	23
Figure 2.6. Analogs with rhodanine methylene substitution.	24
Figure 2.5. Final two analogs compared to 5a and 5f.....	24

LIST OF SCHEMES

Scheme 2.1. Overall synthetic scheme.	14
Scheme 2.2. Free-radical chlorination, diazotization, and Japp-Klingemann.	15
Scheme 2.3. Final two steps.....	16
Scheme 2.4. Japp-Klingemann reaction mechanism.	17
Scheme 2.5. Rhodanine methyl ester synthesis for diversification.....	26

GLOSSARY OF TERMS

α KG	alpha ketogluterate
cLogP	calculated logarithm of partition coefficient
δ	chemical shift
eq	equivalents
FAD	Flavin adenine dinucleotide
h	hour(s)
H(x)K(y)me(z)	histone (x) lysine (y) methyl (z)
HAT	histone acetyltransferase
HDAC	histone deacetylase
HDM	histone demethylase
HMT	histone methyltransferase
HTS	high-throughput screen
IC ₅₀	half maximum inhibitory concentration
ING	inhibitor growth family
JHDM	Jumonji-C domain containing histone demethylase
Jmj-C	Jumonji-C
KDM	lysine specific demethylase
K _i	dissociation constant
LCMS	liquid-chromatography mass-spectrometry
LSD	lysine specific demethylase
M	molar
MAO	monoamine oxidase
MAOI	monoamine oxidase inhibitor
Me	methyl
min	minute
Mmol	millimole
NBS	N-bromosuccinimide
NCS	N-chlorosuccinimide
NMR	nuclear magnetic resonance
Ph	phenyl
ppm	parts per million
rt	room temperature
SAR	structure-activity relationship
TEA	triethylamine
UV	ultraviolet
μ L	microliter

CHAPTER 1 INTRODUCTION

1.1 EPIGENETICS AND THE STRUCTURE AND FUNCTION OF HISTONE PROTEINS

Epigenetics is the study of changes in heritable gene expression without changing the existing genetic code. Different environmental factors can dictate whether genes are expressed or silenced, leading to phenotypic variation. Changes can come about due to various factors, such as an organism's needs within a certain stage of development or the needs of one tissue versus another. To fulfill these needs, changes are made that affect which portions of DNA can be read, essentially turning genes on or off like a light switch. Each human cell contains about two meters of DNA, which must be arranged such that it can be packed into the cell. This is done by histone proteins. Rather than allowing DNA to lie in a straight line, histone proteins package it into a more ordered and compact form called chromatin. DNA coils around an octamer consisting of four pairs of histone protein dimers (H2A, H2B, H3 and H4) to create small groups called nucleosomes with each nucleosome containing about 146 base pairs of DNA,

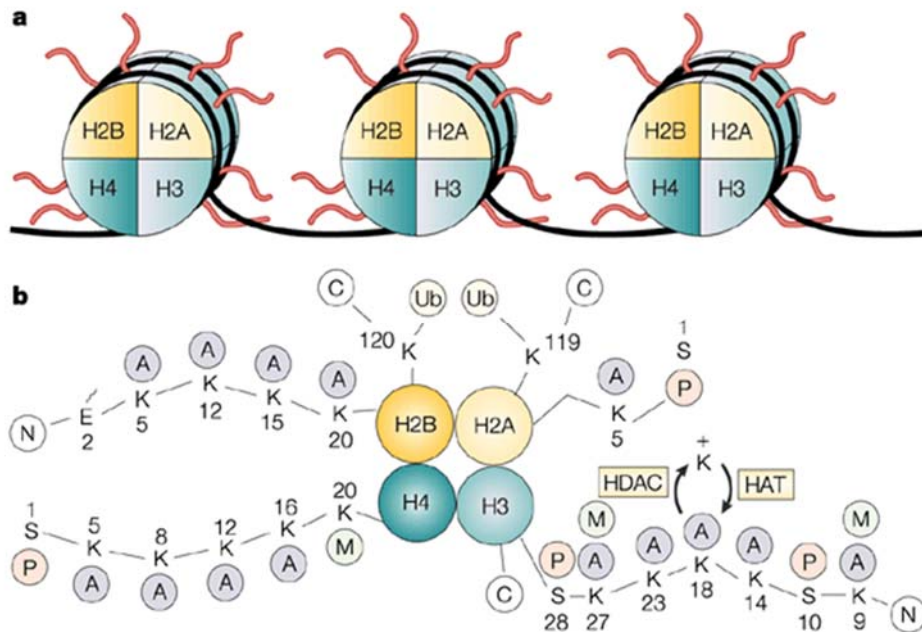


Figure 1.1. Histone arrangement within nucleosome. Reprinted from Cold Spring Harbor Laboratory Press: [*Genes & Development*] Cheng, Z.; Cheung, P.; Kuo, A. J.; Yukl, E. T.; Wilmot, C. M.; Gozani, O.; Patel, D. J. *Genes Dev.* **2014**, *28* (16), 1758–1771.

wrapped in 1.67 superhelical turns (**Figure 1**).¹ Histones H3 and H4 combine to make a central heterotetramer that has two heterodimers of H2A and H2B on either side. Between each nucleosome is a linker of DNA containing anywhere from 10 to 60 base pairs. This series of nucleosomes is further compacted into fibers that are held together by an additional histone that links nucleosome cores together. These fibers are condensed even more into chromatin fibers.² Each histone has a tail that protrudes from the surface and consists of 20-35 mostly basic amino acid residues. While these tails don't play much of a role in stability or nucleosome interactions, they do affect the overall folding of nucleosome groups into higher ordered structures.²

1.2 HISTONE MODIFICATIONS

The way that the DNA is wrapped can affect access to it and thus affect its readability. Histone-DNA interaction can be affected by chemical changes to the histone, such as methylation, acetylation, phosphorylation, and a few others.¹⁻⁵ For example, methyl groups can be installed on histone lysine residues (K) or arginine residues (R) by histone methyltransferases (HMTs) or removed by histone demethylases (HDMs), while acetyl groups can be installed on lysine residues by histone acetyltransferases (HATs) and removed by histone deacetylases (HDACs).¹⁻⁵ Various studies have shown that the patterns of histone modification at specific sites are correlated with certain biological functions, mostly related to transcription events. For example, transcriptional repression in eukaryotes may result from trimethylation of H3K9 in the absence of H3 and H4 acetylation.^{2,6} Additionally, histone modifications are known to function in a cell's response to stress or DNA damage, differentiation of stem cells, and regulation of the cell cycle.^{2,6}

Methylation of H3K4 is generally considered to play an important role in activation of genes because it allows transcription promoters to bind to it. However, it has also been observed that H3K4me2 and me3 are linked to repression of transcription via binding of a co-repressor from the

inhibitor of growth family, ING2. This is useful for situations in which DNA has been damaged and active transcription needs to be immediately halted to prevent proliferation of cells with damaged or altered DNA.⁷

Bernstein et al. note that H3K4me3 and H3K27me3 are opposing regulators of transcription by either recruiting nucleosome remodeling enzymes or promoting a compact chromatin structure, respectively. However, they observed many areas in embryonic stem cells that contained both the activating H3K4me3 mark, as well as the repressive H3K27me3 mark, and subsequently named them “bivalent domains” because they exhibit both activities. In effect, these bivalent domains may prevent expression of genes during development while still leaving the cells primed for differentiation when they are required for a developmental process.⁸

1.3 HISTONE DEMETHYLASES

While histone modifications are necessary for growth and development, aberrant activity of the enzymes that make these changes can cause problems. Histone demethylases are enzymes that can demethylate methylated lysine or arginine residues, the former being more thoroughly studied. Irregular histone methylation/demethylation has been implicated in various cancer types, including but not limited to, lung cancer, prostate cancer, kidney cancer and leukemia.⁹⁻¹² When compared to normal, healthy cells, the histone methylation patterns found in cancer cells are different and it has been suggested that irregular histone methylation patterns play a role in tumorigenesis. It was initially unclear whether changes in global methylation of certain histones is a cause or effect of cancer, but more recent studies have shown correlation with increased reappearance of cancer and mortality rate.⁶ A 2009 study conducted by Elsheikh et al. showed a decrease in global H3 and H4 acetylation and methylation marks in breast tumors with adverse characteristics and poor prognosis, while an increase in these same marks was seen in normal breast epithelial cells or tumors with a good prognosis. This suggests that

demethylation and deacetylation are either a cause or consequence of some cases of breast cancer.¹³ Furthermore, it has been suggested that unusual histone modification patterns correlate with instances of cognitive disabilities. For example, trimethylation of H3K36 has been linked to Sotos syndrome, a genetic disorder that causes excessive growth within the first several years of life, often joined by impaired speech and intellectual impairment ranging from odd obsessions and phobias to impulsive tantrums, among several other debilitating symptoms. Because HDMs and HMTs work with a high degree of synergy, the consequences of their functions vary widely depending on the combination of methylation states (as well as other functional group changes). This means that the methylation of one histone residue may affect a change in its neighbor.

Lysine residues have four methylation states: unmethylated (me0), monomethylated (me1), dimethylated (me2) and trimethylated (me3) (**Figure 1.2**). Changes to these residues tend to be found at H3K4, H3K9, H3K27, H3K36, H3K79 and H4K20. HDMs are divided into two major families, depending on their method of demethylation: the first is a flavin adenine dinucleotide (FAD)-dependent amine oxidase and the second type relies on both Fe(II) and α -ketoglutarate (α KG) to function. Until the 2004 discovery of LSD1 (Lysine Specific Demethylase), it was heavily debated whether histone demethylation could occur at all; instead, the leading hypotheses stated that removal of histone lysine methyl groups came about due to complete turnover of the cell or enzymatic removal of the histone tail.^{6,14} The discovery of

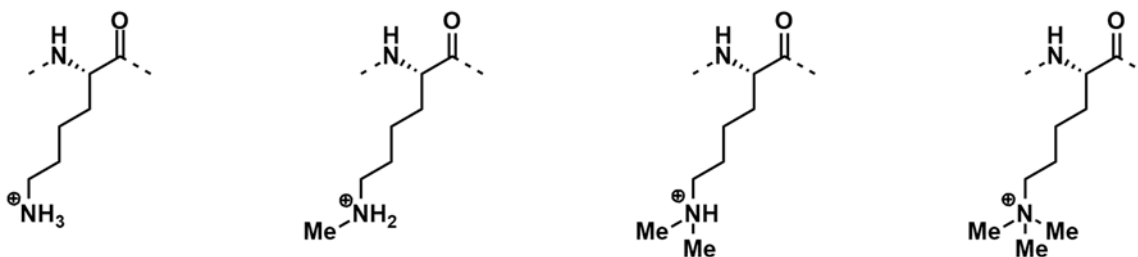


Figure 1.2. Methylation states of lysine residues. Methylation state is indicated by “me0-3” for unmethylated, mono-, di-, or tri-methylated.

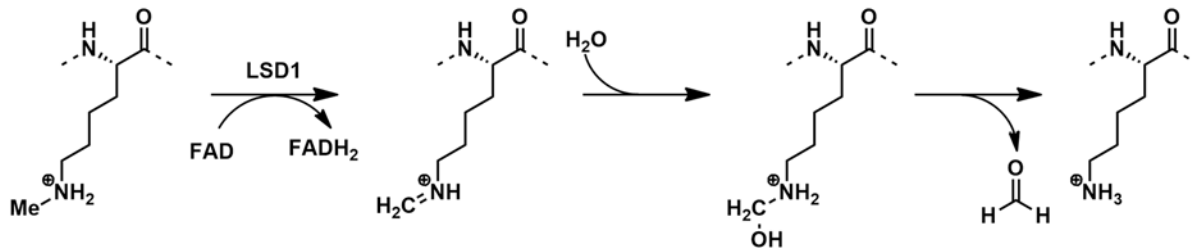


Figure 1.3. FAD-dependent oxidative demethylation mechanism occurring in HDMs that do not contain a Jumonji-C domain.

LSD1 marked the creation of the LSD family of histone demethylases, which was the first of two families.¹⁵ These HDMs catalyze the conversion of methylated lysine to an imine by FAD-dependent oxidation of the α -carbon, which is then hydrolyzed to remove formaldehyde. Because this mechanism relies on the formation of an imine intermediate, the LSD family of HDMs can only demethylate mono- and di-methylated lysine residues (**Figure 1.3**).¹⁵ The demethylases in the second family all include a Jumonji-C domain and are subsequently named Jumonji-C domain containing histone demethylases (JHDMs). The Jumonji-C domain active site contains five residues that bind the Fe(II) and α KG cofactors necessary for function (**Figure 1.4A**). Although some variations have been seen, the active site is fairly

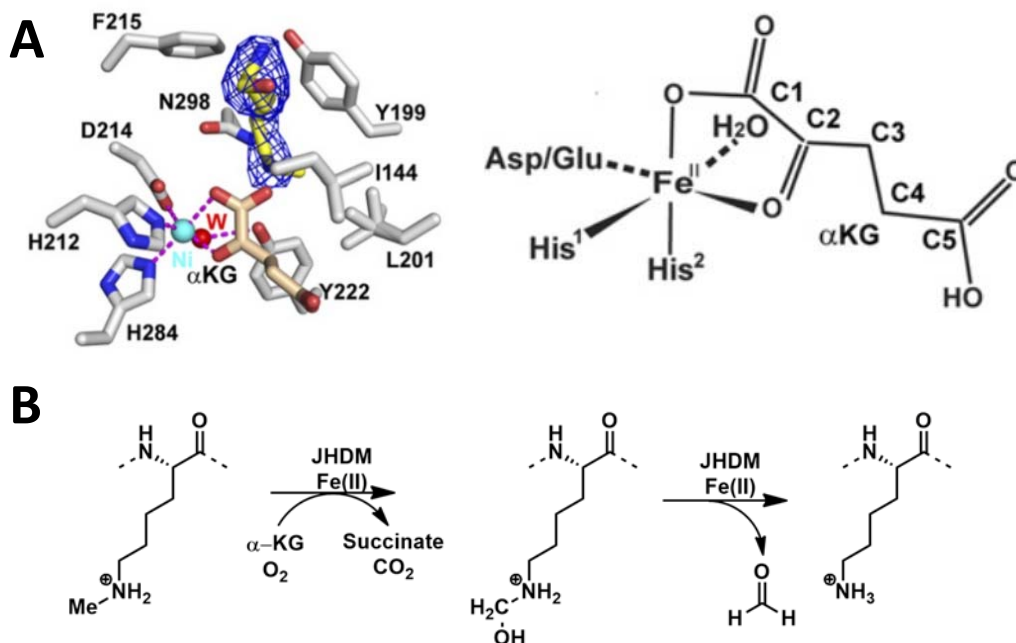


Figure 1.4. Binding and mechanism of JHDMs. (A) JHDM1A mechanism binding α KG and iron. (B) The JHDM mechanism differs from other HDMs by requiring α KG and Fe(II) (B) Reprinted from Cold Spring Harbor Laboratory Press: [*Genes & Development*] Cheng, Z.; Cheung, P.; Kuo, A. J.; Yukl, E. T.; Wilmot, C. M.; Gozani, O.; Patel, D. J. *Genes Dev.* **2014**, 28 (16), 1758–1771.

well conserved within this group.¹⁶ Within the active site, the iron atom is coordinated to three residues: His212, Asp214, and His284 while α KG fits in by coordinating to Fe(II) and is further stabilized by hydrogen bonds to Thr208 and Lys230¹⁷. In closely related JHDMs, the aspartate and threonine residues may be replaced by glutamate and tyrosine residues, respectively.¹⁸

JHDMs catalyze lysine demethylation through a carbinolamine intermediate via radical attack by an oxoferryl species. The unstable carbinolamine spontaneously releases formaldehyde, leaving the demethylated lysine behind (**Figure 1.4B**).¹⁹ The JHDM family is further split into seven different classes, but general mechanistic details remain the same.⁴ JHDMs have been observed to demethylate various lysine residues and methylation states on histones 3 and 4. For example, JHDM1A works on H3K36me1/2, while JHDM2A focuses on H3K9me1/2 and JHDM3 demethylates H3K9me2/3 and H3K36me2/3.^{17,20,21} Methylation state specificity in these enzymes may just be attributed to the different sizes of the active sites across this family.²²

1.4 CURRENT STATE OF HDM INHIBITOR RESEARCH

HMTs and HDMs are essential for proper growth and development throughout all stages of life; it is only when they are over- or under-expressed that they become problematic. LSD1 is essential for the differentiation of cell types, from the embryo all the way through adulthood. During embryo development, LSD1 maintains stem cell pluripotency by policing the relative methylation states of H3K4 and H3K27, which prevents activation of the genes responsible for cell differentiation and when it is time for cell differentiation, LSD1 plays an essential role in withdrawing the related enhancers.^{23,24} For adults, this enzyme is essential for the creation of new blood cells (hematopoiesis).^{25,26}

LSD enzymes fall into a larger superfamily of amine oxidases and, as such, are closely related to monoamine oxidases (MAOs). Because of this, the majority of work in LSD1 inhibition has dealt with known monoamine oxidase inhibitors (MAOIs) and their derivatives. MAOIs block the function of

monoamine oxidase, an enzyme that removes the neurotransmitters norepinephrine, serotonin and dopamine from the brain. When monoamine oxidase is inhibited, the concentration of these neurotransmitters is increased; subsequently, these drugs are used as antidepressants.²⁷ MAOIs work by making an irreversible covalent bond to the enzyme cofactor, FAD. MAO function may only be restored by resynthesizing the whole enzyme.²⁸ While there exist other types, most of research in this area has been focused on the MAOI, tranylcypromine (**Figure 1.5**), and its derivatives. Of note, GlaxoSmithKline has developed the tranylcypromine derivative GSK2879552 (**Figure 1.5**), which is both a selective and potent LSD1 inhibitor that can be delivered orally. Growth inhibition studies showed that this compound exhibits antitumor effects by inhibiting/halting tumor growth in small cell lung carcinoma and acute myeloid leukemia and it is now in phase I clinical trials for both cancer types.^{26,29,30}

ORY-1001 (**Figure 1.5**), from Oryzon, is another potent inhibitor that is more than 1,000-fold selective for LSD1 over LSD2 and MAOs. At extremely low doses, ORY-1001 has shown marked reduction in tumor growth in rats. It has also been observed that this compound is sufficiently bioavailable when

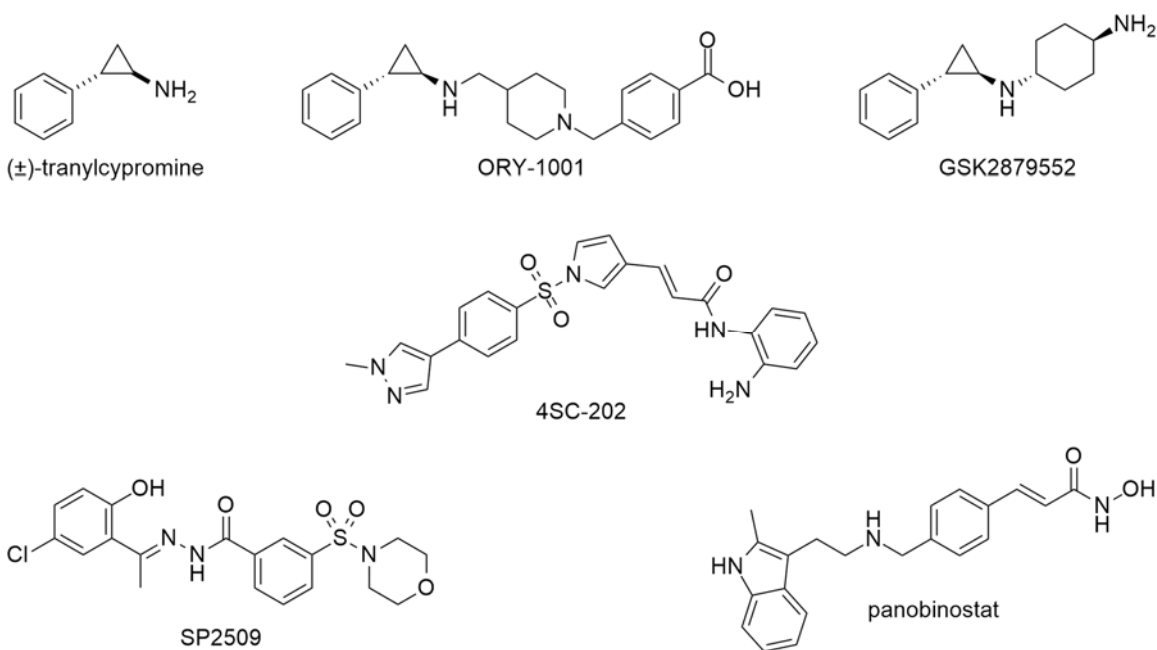


Figure 1.5. HDM inhibitors in active clinical trials.

delivered orally, a property that is not shared by the majority of HDM inhibitors. ORY-1001 is currently in phase I/IIA clinical trials for patients with acute leukemia.

As it turns out, combinatorial therapy involving HDM inhibitors paired with HDAC inhibition may be an effective method of tumor suppression. 4SC-202 (**Figure 1.5**) is a potent inhibitor of LSD1, as well as HDACs 1-3, while another compound, SP2509 (**Figure 1.5**), is being used in combination with panobinostat (**Figure 1.5**), a pan-HDAC inhibitor. Each of these compounds are in phase I clinical trials for advanced hematological malignancies and acute myeloid leukemia, respectively.

Progress in pharmaceutical HDM inhibitor study is certainly beginning to gain momentum, but when it comes to therapeutic JHDM inhibition, research is still in the early phases. The issue lies in the similarity of the enzymes in this class because they all contain the highly conserved Jumonji-C catalytic domain making it quite difficult to achieve proper selectivity. Although there have been a number of demethylase inhibitors reported in the last decade, only a handful of these are promising in regard to JHDM-class specificity. In fact, the first inhibitor specific to JHDMs, GSK-J1, was just reported in 2012. GSK-J1 (**Figure 1.6**) specifically inhibits the demethylases in the KDM6 class with a mild inhibitory effect on the KDM5 class and takes advantage of multiple features within the KDM6 active site. The propionic acid acts as an α KG mimic to bind with Lys, Thr, and Asn residues while the tetrahydrobenzazepine fills a hydrophobic pocket, sandwiched between an Arg and a Pro residue.³¹ This allows it to bind competitively with regard to α KG, but non-competitively with the peptide substrate.

IOX1 (**Figure 1.6**) is a hydroxyquinoline-based, broad-spectrum inhibitor discovered through a high-throughput screen that identified various hydroxyquinolines as inhibitors of KDM4E. This compound binds the active site by chelating Fe(II) in a bidentate manner via the pyridinyl nitrogen and the phenol while the carboxylate interacts with active site residues.³² Like many of the reported

inhibitors, this compound experienced permeability issues which were overcome by converting it to the n-octyl ester at the cost of a minor potency decrease.

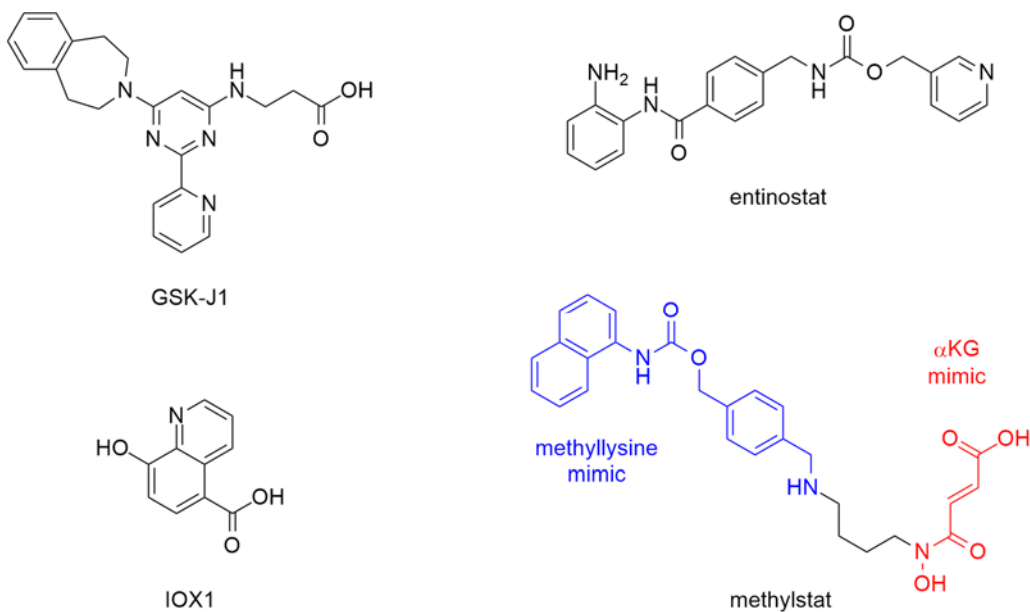


FIGURE 1.6. Previously identified inhibitors of JHDMs. GSK-J1 mimics α KG, allowing it to bind in the Jumonji-C domain active site. IOX1 is a bidentate metal chelator that binds to Fe(II) in the active site. Methylstat is also an α KG mimic, but differs from GSK-J1 in that it also contains a methyllysine mimic which is connected by a four-carbon linker allowing optimal placement within the active site.

The Wang Lab developed methylstat (**Figure 1.6** and **Figure 1.7**), a bivalent, broad-spectrum Jmj-C KDM inhibitor consisting of a methyllysine mimic and an α KG mimic connected by a 4-carbon linker, which allows binding similar to the native substrates of the enzyme. It displayed low micromolar IC_{50} (the concentration of compound at which 50% of the enzyme activity is inhibited) values for KDM4A (4.3 μ M), KDM4C (3.4 μ M), KDM4E (5.9 μ M) and a relatively low IC_{50} for KDM6B (43 μ M), as well as a sub-micromolar IC_{50} for JHDM1A (900 nM).³³ Methylstat displayed no activity in LSD1 or the HDACs that were evaluated and this compound is unique in the fact that it was designed as a bivalent inhibitor to mimic both KDM substrates (α KG and methyllysine), rather than just one. Methylstat's methyllysine mimic, inspired by the histone deacetylase (HDAC) inhibitor, Entinostat, is separated from the α KG mimic by a 4-carbon linker analogous to the spacing of the native substrates. As with the previous example, IOX1, methylstat needed to be converted to the ester to overcome the permeability obstacle.

Next, the Wang lab created methylstat^{fluor} (**FIGURE 1.7**), a fluorescent tracer for use in fluorescence polarization assays. This fluorescent probe allowed the K_i (binding affinity) of α KG and JHDM1A to be measured for the first time ever. It was also used to evaluate the binding constants of several non-fluorescent molecules that bind in the JHDM1A active site. Most importantly, methylstat^{fluor} was used to develop a highly robust assay for high-throughput screening (HTS) to discover novel JHDM inhibitors.³⁴ In addition to the methylstat^{fluor}, an affinity probe (**FIGURE 1.7**) was developed to use for pulldown assays, which would allow JHDMs to be pulled from complex mixtures.³⁵

Development of chemical probes to study the structure and function of HDMs is critical for understanding the nuances of each enzyme and, ultimately, to stop or prevent deviant activity. They can be functionalized for different roles, such as fluorescent probes for visualizing bound HDMs or affinity

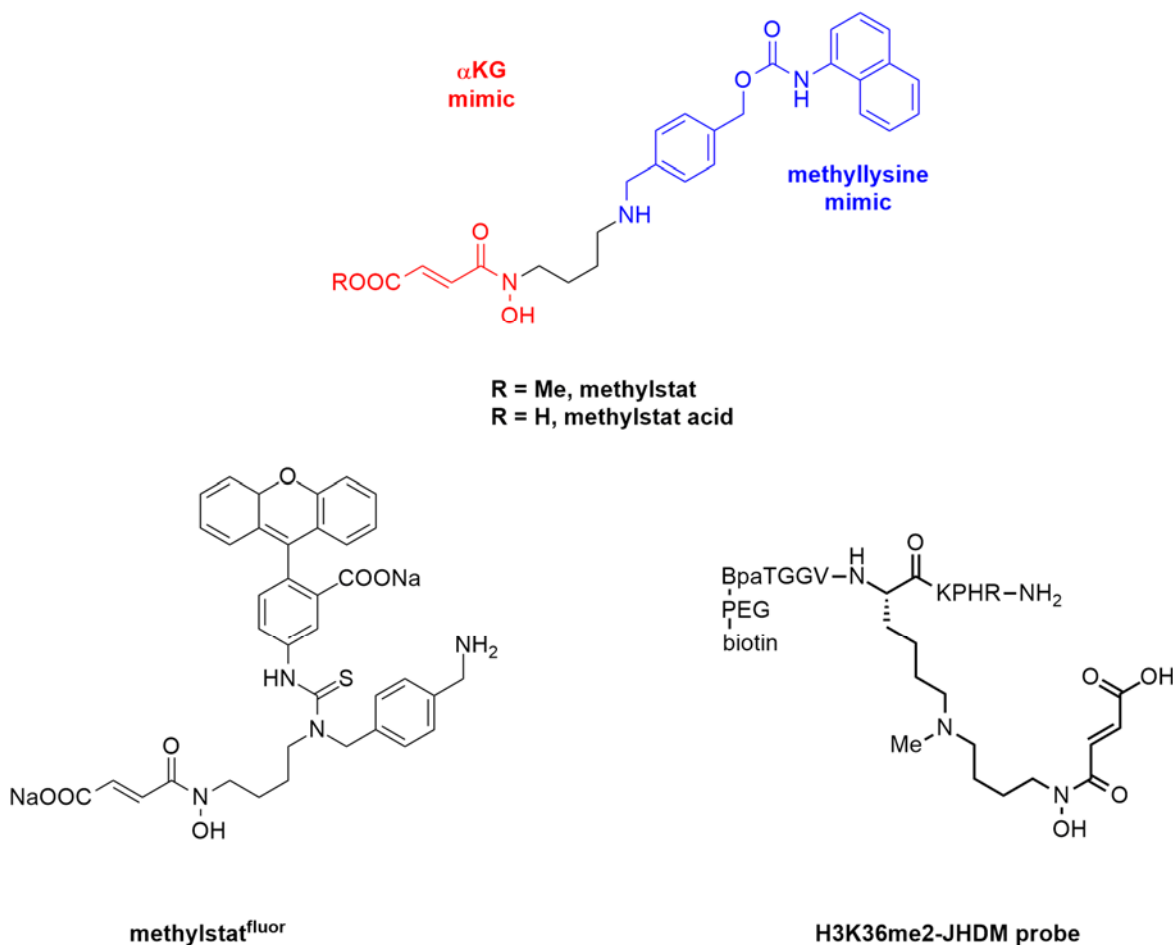


Figure 1.7. Methylstat and methylstat probes developed by the Wang lab.

probes to collect HDMs from a complex mixture of proteins. They can even become leads for pharmaceutical development. Because many JHDM inhibitors are substrate mimics, it is difficult to gain specificity for one JHDM over another. New scaffolds may be the key to discovering inhibitors that can selectively inhibit a small subset or, ideally, just a single demethylase which can allow the study of specific methylation patterns and their effects in gene expression, roles in disorders and diseases, and potentially develop advanced treatments for genetic anomalies.

CHAPTER 2 STRUCTURE-ACTIVITY RELATIONSHIP STUDY

2.1 DISCOVERY OF A UNIQUE JHDM1A INHIBITOR

Many existing HDM inhibitors are simple substrate mimics that imitate a chelator, α KG or both a chelator and α KG. While these inhibitors work for their intended purpose of generally stopping HDMs from functioning, specificity in JHDMs is all but nonexistent. Thus, the need for new cores from which to build HDM inhibitors cannot be overstated, but where do we begin? An attractive starting point is high-throughput screening of libraries of known compounds because it allows a large number of compounds from diverse structural classes to be screened for a certain threshold of activity in the desired target. To this end, the Wang Lab conducted a high-throughput screen (HTS) of the Maybridge library (14,400 compounds) against JHDM1A in the presence of methylstat^{fluor}, the fluorescent tracer designed by the same lab.³⁶ The screen generated 258 hits, 100 of which were chosen for a counter-screen designed to rule out false positives. The immunofluorescence counter-screen assay was conducted using HeLa and MiaPaCa2 cells treated with various concentrations of the chosen 100 compounds, using methylstat acid and DMSO for positive and negative controls, respectively. This screen looked for an increase in the cellular levels of the H3K36me2, which would indicate demethylase inhibition activity. This epigenetic mark was chosen because it is known to be demethylated by JHDM1A. Five compounds survived this screen, but only four could be appropriately identified; the K_i (binding constant) and IC_{50} (concentration at which 50% inhibition is observed) in JHDM1A and JMJD2A were measured for each of these four compounds using a novel *in-vitro* fluorescence-polarization-based competition binding assay that the Wang lab developed.³⁶ The fifth compound was unable to be identified spectroscopically, as it may have decomposed in the well plate. One of the four initial hits did not show any binding affinity toward either protein at any concentration and was ultimately determined to be a false positive. This left three compounds of interest: JFD02841, NRB00125 and HTS12214 (**Figure 2.1**); the compound names were

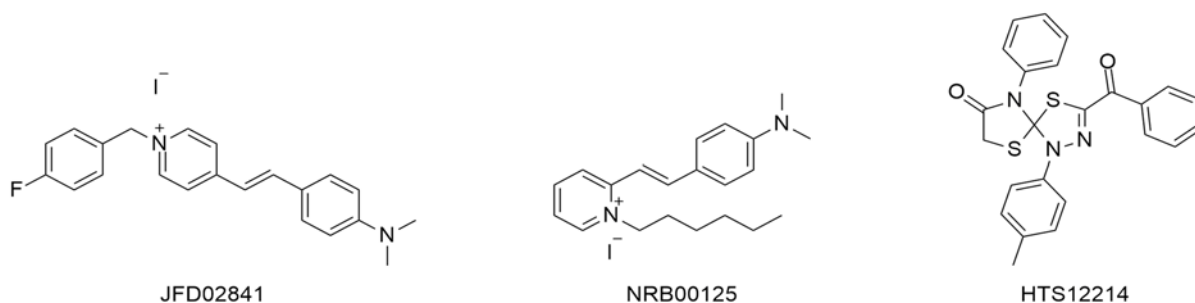


Figure 2.1. Structures of JHDM1A inhibitors discovered from high-throughput screening of the Maybridge library. HTS12214 is particularly interesting for its unique skeleton.

taken from their designation within the Maybridge library). The compounds were then evaluated (at concentrations ranging from 25 nM to 50 μ M) by a second cell-based immunofluorescence assay in the

	JHDM1A K_i (μ M)	JHDM1A (H3K9me3) EC_{50} (μ M)	JHDM1A (H3K36me2) EC_{50} (μ M)
α KG	0.185	N/A	N/A
Methylstat	0.0113	1.18	0.96
NRB00125	0.28	0.66	0.28
JFD02841	0.41	3.96	1.26
HTS12214	1.5	0.9	0.93

Table 2.1. Activity of inhibitors discovered in the Maybridge library. Activity and binding of JHDM1A inhibitors found in the Maybridge library, as well as its native substrate, α KG. Data was obtained by fluorescence polarization competition binding and immunostaining.

presence of JHDM1A looking for an increase in overall methylation of H3K36me2 within a cell. HTS12214 was the least potent and didn't bind as well as the others

(**Table 2.1**; K_i s of 1.50 μ M and 3.02 μ M toward

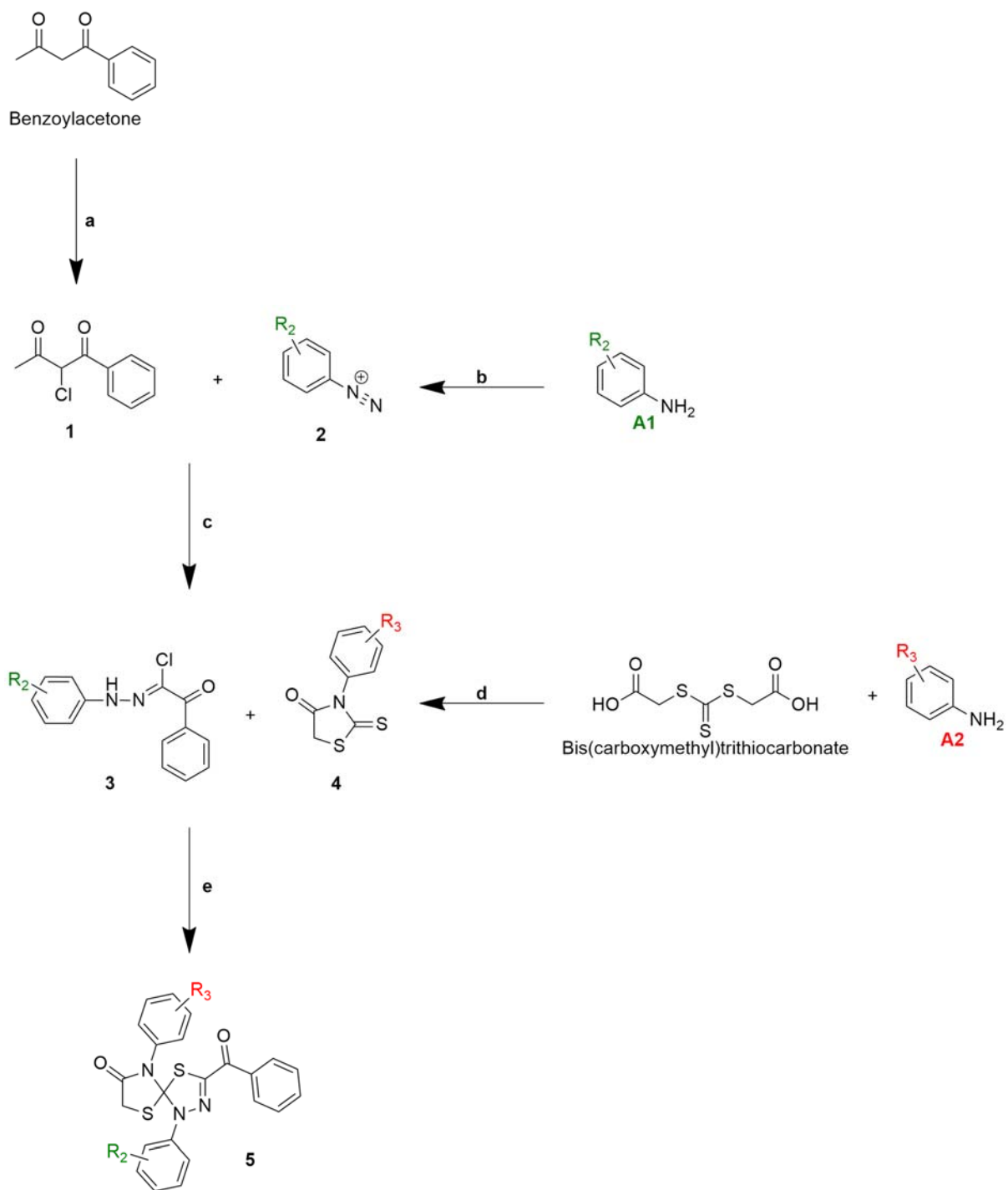
JHDM1A and JMJD2A, respectively) but it is structurally

distinct from Methylstat.^{34,36} In fact, it is different from all known JHDM inhibitors.

2.2 NEW SPIROCYCLE "HIT" COMPOUND

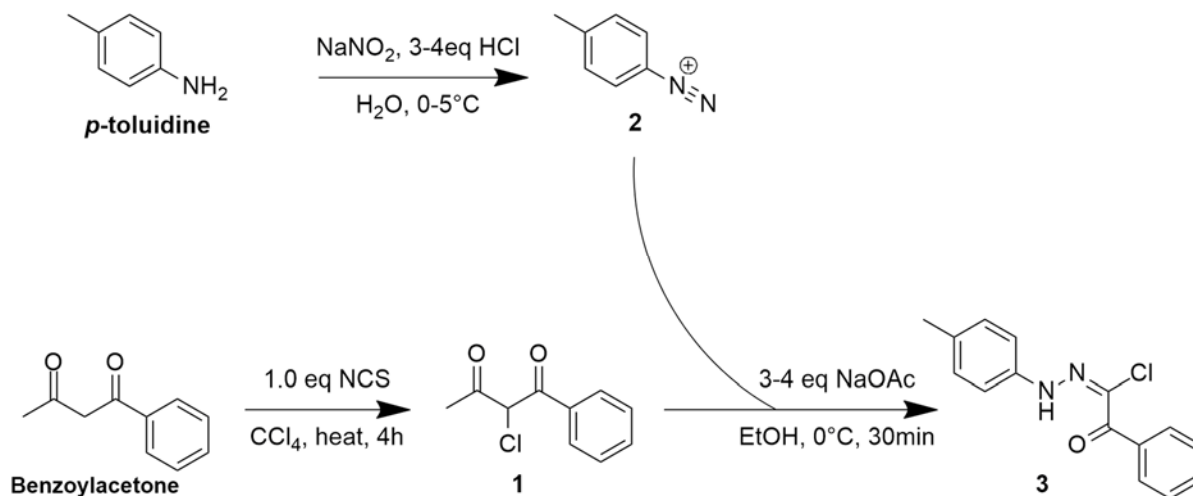
HTS12214 is a spirocyclic compound consisting

of two five-membered heterocycles sharing one, asymmetric carbon. The major important feature of its structure is that it has 3 aromatic rings pointing in different directions; it's possible that this is responsible, in part, for the observed activity in JHDM1A as each aromatic section could feasibly fit into its own hydrophobic space in the enzyme's binding pocket. The majority of the functionalization we studied consisted of altering the aromatic ring substitutions, mostly in the R_2 and R_3 positions. The synthetic route that was used (**Scheme 2.1**) does not utilize any chiral catalysts and thus it produces a racemic mixture so enantiomeric excess (e.e.) was not measured.



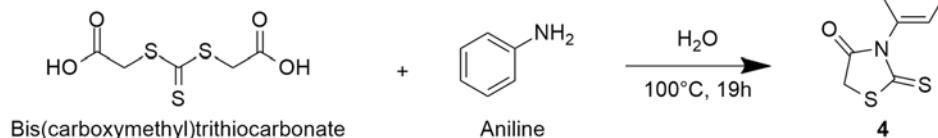
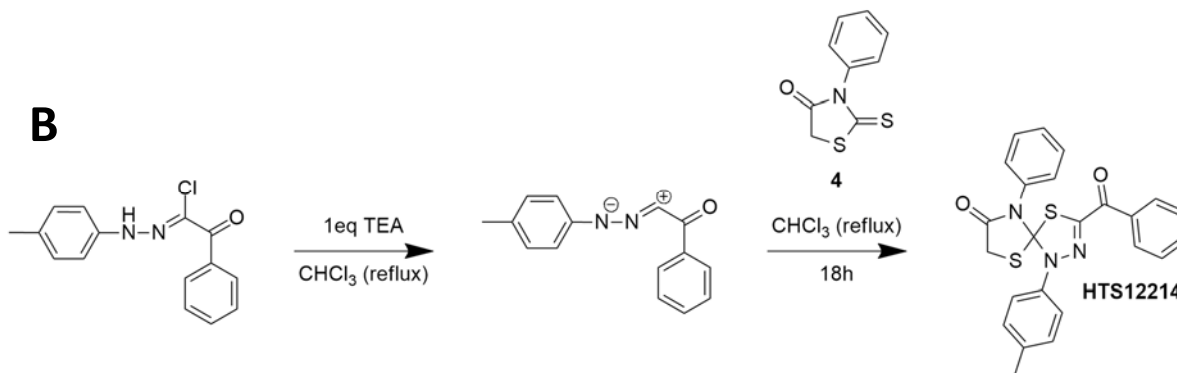
Scheme 2.1. Overall synthetic scheme. Variation was achieved by using different commercially available anilines. Reagents and conditions: **a**) Benzoylacetone (1.0 equiv), NCS (1.0 equiv), CCl_4 , reflux, 4h, 88%; **b**) **A₁** (1.0 equiv), NaNO_2 (1.0 equiv), HCl (3.0-4.0 equiv), water, 0 °C, 5 min, 77%; **c**) **1** (1.0 equiv), NaOAc (1.6 equiv), ethanol (0.2M), 0 °C, add **2** (1.0 equiv), 20-60 min, 77%; **d**) bis(carboxymethyl)trithiocarbonate (1.1 equiv), **A₂** (1.0 equiv), water, reflux, 18 h, 94%; **e**) **3** (1.2 equiv), **4** (1.0 equiv), TEA (1.1 equiv), chloroform, reflux, 18 h, 22%.

The purpose of this study was to tune the potency and binding of this new scaffold in JHDM1A by studying the structure-activity relationship (SAR). I decided to first verify the plausibility of my chosen route by synthesizing the hit compound, HTS12214, then evaluate biological activity. I began by free-radical chlorination of benzoylacetone using NCS to make **1** in 88% yield (**Scheme 2.1** & **Scheme 2.2**).³⁷ This was combined with 4-methylbenzenediazonium, **2**, (prepared from commercially available *p*-toluidine) in the presence of base to give hydrazone **3**, via a Japp-Klingemann reaction.³⁸



Scheme 2.2. Free-radical chlorination, diazotization, and Japp-Klingemann.

Aniline was combined with bis(carboxymethyl)trithiocarbonate to yield *N*-phenylrhodanine **4** in quantitative yield. Because the bis(carboxymethyl)trithiocarbonate starting material was difficult to separate from the desired product, **4**, this reaction was done with a slight excess of aniline (1.2 equiv) which was easily washed away in the workup. The rhodanine derivative produced in this step was combined with hydrazone **3** in a base catalyzed 1,3-dipolar cyclization to give the desired spiro-compound.^{39,40} To make purification easier, 1.2 equiv of **3** was used in final step as **4** often had a very similar R_f to the desired product. This reaction was still fairly messy and 20-25% yield was seen after purification. The poor yield may be due to overheating and it is possible that this reaction does not require heating to reflux (60°C). I attempted the reaction at room temperature, but observed no product formation.

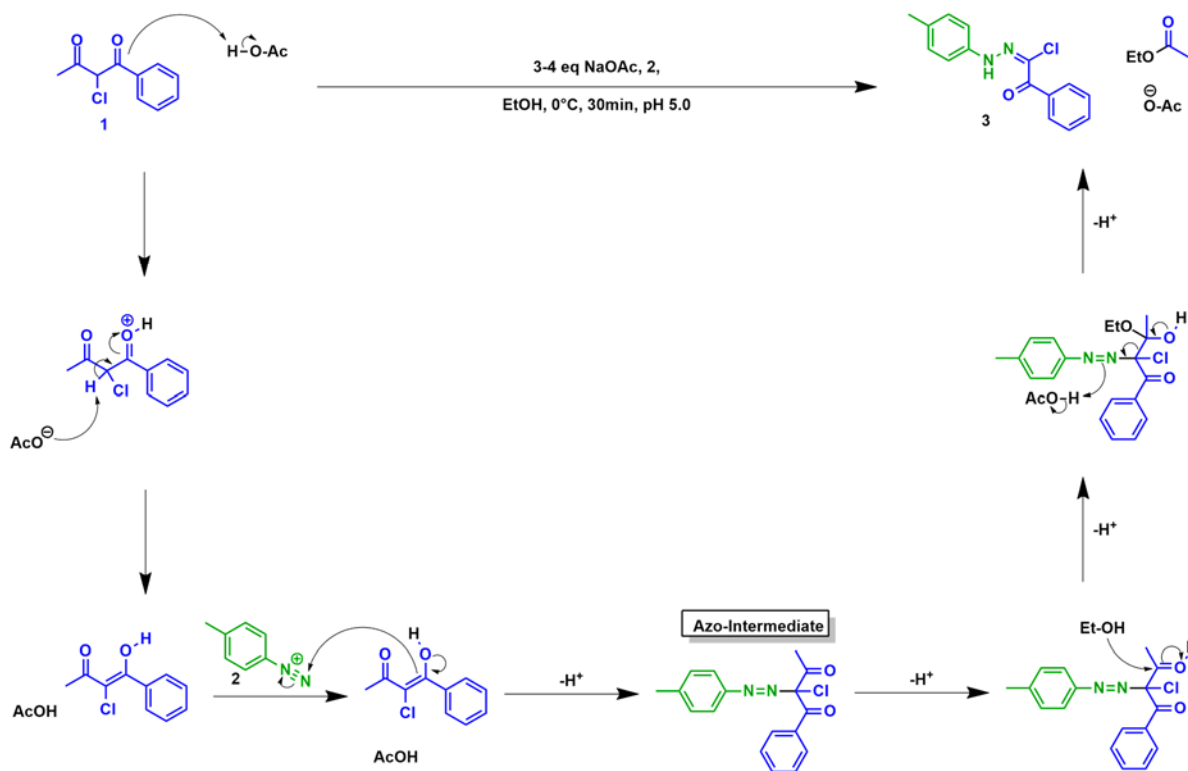
A**B**

Scheme 2.3. Final two steps. A) N-arylrhodanine synthesis via nucleophilic cyclization. B) 1,3-dipolar cyclization to yield desired spirocycle.

2.3 SYNTHETIC HURDLES

While this route did permit synthesis of the desired product while allowing for diversification, it was, in some cases, severely limited by the Japp-Klingemann step. This reaction sometimes produced up to 77% yield, but the yield was often very low (below 20%). There are two major contributors to this: the first is that the reaction yields two hydrazone products and the second contributor is the type of aniline aryl substitution. Additionally, many recent sources were unclear as to the seemingly minor details of the reaction, such as the suggested pH, which had a strong effect on the outcome. The Japp-Klingemann reaction was discovered in 1887 when F.R. Japp and F. Klingemann were attempting to prepare an azo ester by coupling benzenediazonium chloride with ethyl-2-methylacetoacetate sodium, but this dated method proved to be a nuisance from day one. They observed that their product contained two fewer carbons than intended and turned out to be the phenylhydrazone. While this very old method can be (and is) used to prepare very colorful azo-compounds if the pH remains low enough, conversion to a hydrazone can be achieved by allowing the reaction to become less acidic (pH ~5).⁴¹ I had the additional

requirement of preventing extreme basicity so that I would avoid displacing the dione chlorine. The diazotization step is done in acidic conditions that is later buffered by the basic conditions in the Japp-Klingemann stage. ^1H NMR confirmed that complete conversion to the diazoaniline was achieved within five minutes, so the issue must lie in the Japp-Klingemann step.



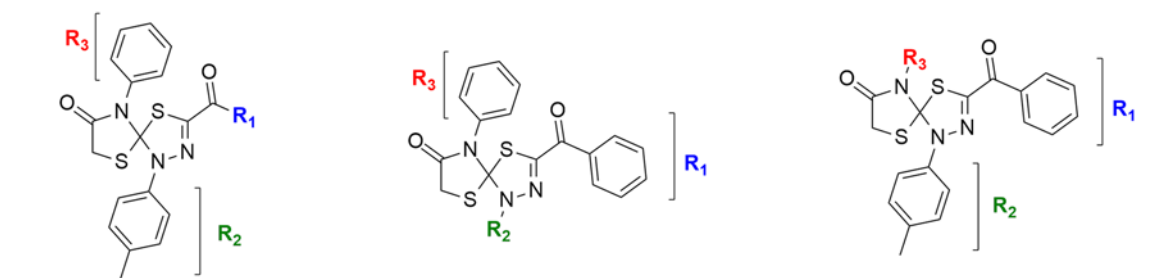
Scheme 2.4. Japp-Klingemann reaction mechanism.

Kürti and Czako report that the aliphatic acyl group will be preferentially cleaved when a mixed β -diketone containing an aliphatic and aromatic acyl group, but I did not always observe this.⁴¹ This seems to be mostly true when the diazoaniline had an alkyl or electron-withdrawing aryl substitution. However, when the diazoaniline contained one or more electron-donating groups on the aromatic ring, the reaction favored formation of the acyl hydrazone rather than the desired aryl hydrazone, if conversion to the hydrazone occurred at all. This is the main contributing factor causing the low yields associated with this reaction when using electron-rich anilines and it was initially difficult to see this via

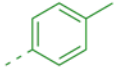
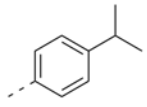
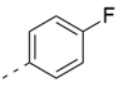
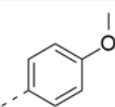
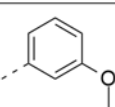
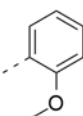
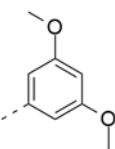
¹H NMR as the chemical shift of the singlet for the benzoylacetone methyl group ($\delta = 2.55\text{ppm}$) is close to the shift of the corresponding methyl group found in the undesired hydrazone ($\delta = 2.0\text{-}3.0\text{ppm}$). Additionally, LCMS could not be used due to the extreme hydrophobicity of the products. When the aromatic substitution was any mono- or di-methoxy group, the observed yield was consistently 15% or less. In some cases, some of the azo-intermediate could be isolated, but because this reaction was often on a smaller scale, attempting to convert it to the desired product failed to produce enough of the aryl hydrazone to isolate. When *N,N*-dimethylaminoaniline was used in this reaction, it stopped at the azo-intermediate. Complete conversion to the azo-intermediate was achieved and I was able to isolate it. I attempted to force conversion via several reported procedures (heat, stronger base, 10% phosphoric acid, glacial acetic acid) but was unsuccessful.^{42,43} On the plus side, this undesired azo-compound is a pleasant, bright magenta, so that made the low yield a little less depressing. In the future, one might try to synthesize this compound by using 4-nitroaniline for the Japp-Klingemann step, then reduce the nitro group using zinc dust and ammonium chloride (via the hydroxylamine intermediate).⁴⁴

In an attempt to avoid formation of the undesired acyl-hydrazone, 3-chlorobenzoyl acetone was replaced with the corresponding symmetric 3-chloro-diphenyl dione, but this compound did not react with the diazoaniline at all. Additionally, benzoylacetone could be replaced by ethylbenzoylacetate, which was reported by Heath-Brown and Phillpot to give the desired hydrazone in favorable yield with *p*-anisidine, but this reagent is significantly more expensive.⁴² Another possible solution is doing the Japp-Klingemann reaction prior to halogenation to give the corresponding hydrazone which can then be chlorinated or brominated with NCS or NBS, respectively, to achieve the desired product.⁴⁵ This last method may increase the rate and amount of conversion in the Japp-Klingemann reaction because there is less steric hindrance due to the absence of the large chlorine atom.

2.4 DATA AND DISCUSSION



	R ₁	JHDM1A K _i
5a		4.95 μM
5b	Me	45.05 μM

	R ₂	JHDM1A K _i
5a		4.95 μM
5c		4.02 μM
5d		3.23 μM
5e		8.79 μM
5f		0.41 μM
5g		4.65 μM
5h		11.0 μM
5i		4.57 μM

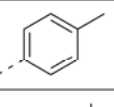
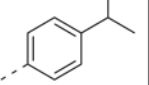
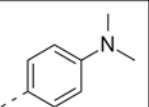
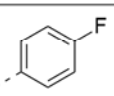
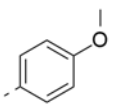
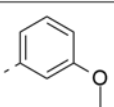
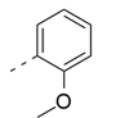
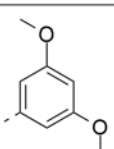
	R ₃	JHDM1A K _i
5a		4.95 μM
5j	H	11.87 μM
5k	Me	3.33 μM
5l		3.33 μM
5m		2.79 μM
5n		17.95 μM
5o		3.37 μM
5p		2.17 μM
5q		1.32 μM
5r		1.92 μM
5s		1.62 μM

Table 2.2. R₁-R₃ substitutions and observed binding constants in JHDM1A.

2.4.1 R₁-SUBSTITUTIONS

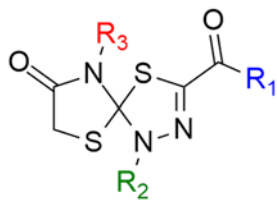


Figure 2.2. Sites of variation.

To optimize the binding of HTS12214, a structure-activity relationship study was conducted by evaluating different substitutions on each of the aromatic rings (**Figure 2.2**). The compounds were evaluated by Dr. Wei Wang using the previously described fluorescence-polarization-based competition binding assay developed by the Wang lab.³⁴ I began by synthesizing the hit compound, **5a**, as well as an analog where the R₁ aryl group was removed, leaving an acyl group. As it turns out, removing the aryl group from R₁ substantially reduces binding from 4.95 μ M for **5a** to 45.05 μ M for acyl analog **5b** (**Table 2.2**). Modeling both compounds in the JHDM1A active site gives potential insight as to why this phenyl ring is crucial for binding. The R₁ phenyl group fits into a hydrophobic space in the binding pocket, anchoring it into place; removing this substitution essentially removes the anchor.

2.4.2 R₂-SUBSTITUTIONS

To vary the aryl substitution in the R₂ position, I used different diazoniums in the Japp-Klingemann step. I first chose to compare four different *para*-substitutions: fluorine, methoxy and unsubstituted phenyl (R₂ = methyl in **5a**). There was no significant change in activity when the aryl substitution was removed (**5c**, K_i = 4.02 μ M). However, adding *p*-fluoro (**5e**, K_i = 8.79 μ M) to this position decreased the activity about two-fold and *p*-methoxy (**5f**, K_i = 0.41 μ M) caused a 12-fold increase in activity. While this was good news, it should be noted that the *p*-fluoroaniline provided significantly increased yield in the Japp-Klingemann reaction in comparison to the *p*-methoxyaniline, which consistently yielded less than 10%. It was unclear as to whether the observed activity changes were due

to a change in size/shape of the compound or if there are electronic effects at work here. The difference in binding between **5a** and **5e** suggests the latter because the Van der Waals radius of fluorine is between that of methyl and hydrogen (~75% that of a methyl group) so its affinity should have been more similar to **5a** and **5c**.⁴⁶

I was curious to see if the activity was related to overall electronics, position of the substitution or both, so I chose different anisidines that essentially allowed me to “walk” the methoxy group around the aromatic ring to evaluate the effect on position and a 3,5-dimethoxy aryl group was chosen as a more electron-rich substitution than the others. *N,N*-dimethylaminoaniline was also chosen for this position, with isopropyl aniline for comparison, but unfortunately, the aminoaniline did not agree with the Japp-Klingemann reaction, preventing synthesis of this analog.

When the **R₂** aryl-substitution was replaced with an isopropyl group, binding increased nearly two-fold (**5d**, $K_i = 3.23 \mu\text{M}$) in comparison to the lead, so it is possible that the substitutions in this position are merely filling space rather than making an electrostatic interaction. To reinforce this idea further, weaker binding was observed as the methoxy group was moved around the ring, closer to the core for the para (**5f**), meta (**5g**), and ortho (**5h**) substitutions, $0.41 \mu\text{M}$, $4.65 \mu\text{M}$, and $11.0 \mu\text{M}$, respectively. Adding a second methoxy to the other meta position (**5i**) caused no change in comparison to the single meta-substitution. Based on this portion of the SAR, it is apparent that the aryl group is necessary and binding is augmented by methoxy substitution in the *para*-position. This substitution is likely filling a hydrophobic space, so it would be interesting to synthesize an analog that contains an alkyl or cycloalkyl substitution here, as a direct comparison.

2.4.3 R₃-SUBSTITUTIONS

R₃ was diversified by using different anilines in the rhodanine cyclization reaction (Scheme 2.3A). Because I already had the anilines available, I decided to begin by comparing the same four substitutions to this position that were made in the R₂ position: fluorine, methoxy and methyl (R₃ = unsubstituted in 5a). Activity increased when R₃ was *p*-methoxy (5p), but decreased when a methyl or fluorine was placed here (5l and 5o, respectively). I then wanted to see how activity would be affected by removing the ring altogether or replacing it with a methyl group (5j and 5k). Replacing the aromatic ring with a methyl group caused a negligible increase in activity and placing a hydrogen here resulted in a three-fold reduction, so it became obvious that the aromatic ring was beneficial and the electron-rich aromatic *p*-methoxy, 5p, was best ($K_i = 2.42 \mu\text{M}$), but it was unclear if the aryl-substitution was making a specific electrostatic interaction or just functioned to fill space in the active site. Of course, to keep the molecular weight of this compound low, the *N*-methyl substitution may be the best option. Interestingly, when R₂ is *p*-methoxy and R₃ is hydrogen or methyl, the K_i is lower in comparison to the corresponding analogs where R₂ is *p*-methyl (Figure 2.3). This is significant when one considers the fact that the R₂ *p*-methoxy analogs tended to perform better than most others.

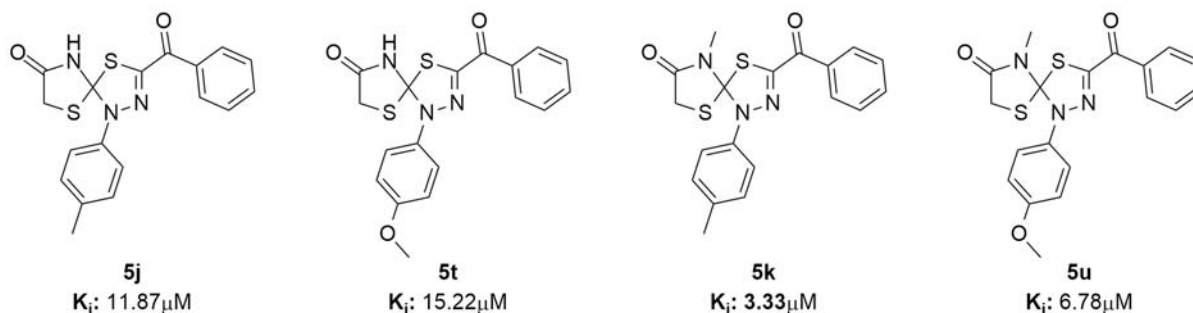


Figure 2.3. Analogs with methyl and unsubstituted rhodanine.

To see if the observed change in activity was related to electronics or an electrostatic interaction, I chose to use the same five anilines I'd used to evaluate R₂. For this position, 4-amino-*N,N*-dimethylaniline (5n) was chosen as a stronger electron-donating group, while 4-isopropylaniline (5m) was chosen as a direct comparator. The isopropyl group, 5m, was substantially superior to the amine,

exhibiting six-fold stronger binding ($K_i = 2.79 \mu\text{M}$ and $17.95 \mu\text{M}$, respectively). This suggests that no electrostatic interaction is occurring and if this substitution is just filling a hydrophobic space, then *para*-methoxy is not only the best, with a K_i of $2.17 \mu\text{M}$, but it is the largest tolerated group for this position.

Additionally, the methoxy group was assessed in the *ortho*- and *meta*-positions of the aromatic ring (**5r** and **5q**, respectively) and 3,5-dimethoxyphenyl (**5s**) was chosen to evaluate the effect, if any, of increased aromatic electron density. All three of these substitutions performed similarly, ranging from 1.32 - $1.92 \mu\text{M}$, with *m*-methoxy (**5q**) being the most potent substitution in this position across all analogs tested. The similar activity for all **R**₃-methoxy analogs indicates that electronics may play a small part in binding as changing the position of the substitution yielded no change.

2.4.4 RHODANINE METHYLENE SUBSTITUTIONS

The rhodanine methylene was also explored as a variation site via aldol condensation. NH_4OH and benzaldehyde were used to synthesize the benzylidene analog (**4a**, **Figure 2.6**); Russel et al. reports that this reaction, with similar starting materials, yields 95% of the desired (*Z*)-stereoisomer.⁴⁷ The propenylidene analog (**4b**, not shown) was created using just NH_4OH in acetone. Substitution in this position did not make a significant change to the observed activity (**Figure 2.4**). I had originally envisioned this site as a place to attach some sort of linker for specific biological assays, such as fluorescence polarization. However, I later discovered that the majority of these compounds fluoresce yellow or green under long-wave UV light (365 nm). This fortunately makes them easy to locate after purification by flash chromatography.

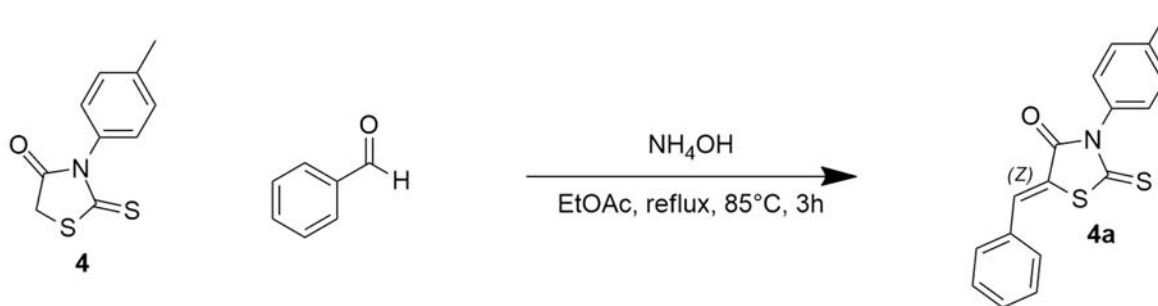


Figure 2.4. Aldol condensation of rhodanine derivatives.

It should be noted that these two analogs were synthesized with the *p*-toluidine rhodanine piece, but the methyl substitution did not change the activity in other analogs and thus these two are comparable to those that contain the phenyl substituent here (Figure 2.5).

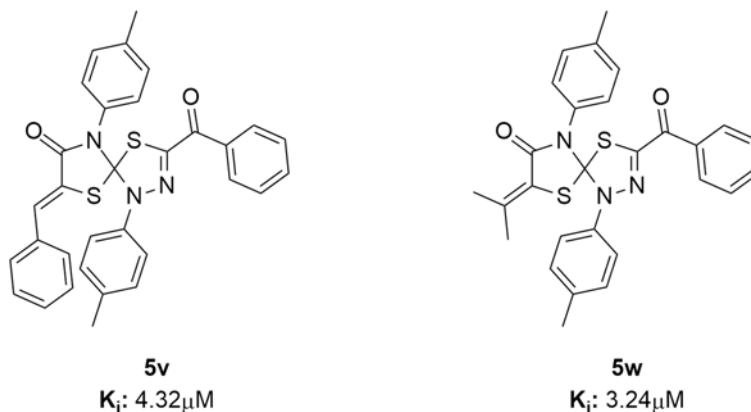


Figure 2.5. Analogs with rhodanine methylene substitution.

2.5 FINAL ANALOGS

To complete this SAR, two final analogs were synthesized. These compounds consisted of the best substitutions, R_1 = phenyl, R_2 = *p*-methoxy, and R_3 = *m*-methoxy (5x) or 3,5-dimethoxy (5y). Although each single substitution yielded a large benefit to binding over 5a, these final two compounds showed that the binding is unfortunately not better than the sum of its parts and while they both performed better than all others in this series, the difference is negligible when compared to 5f (Figure 2.6).

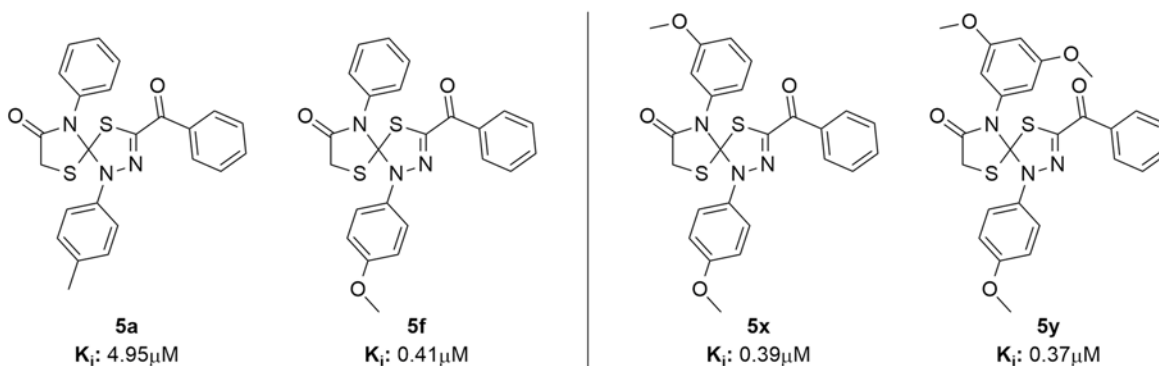


Figure 2.6. Final two analogs compared to 5a and 5f.

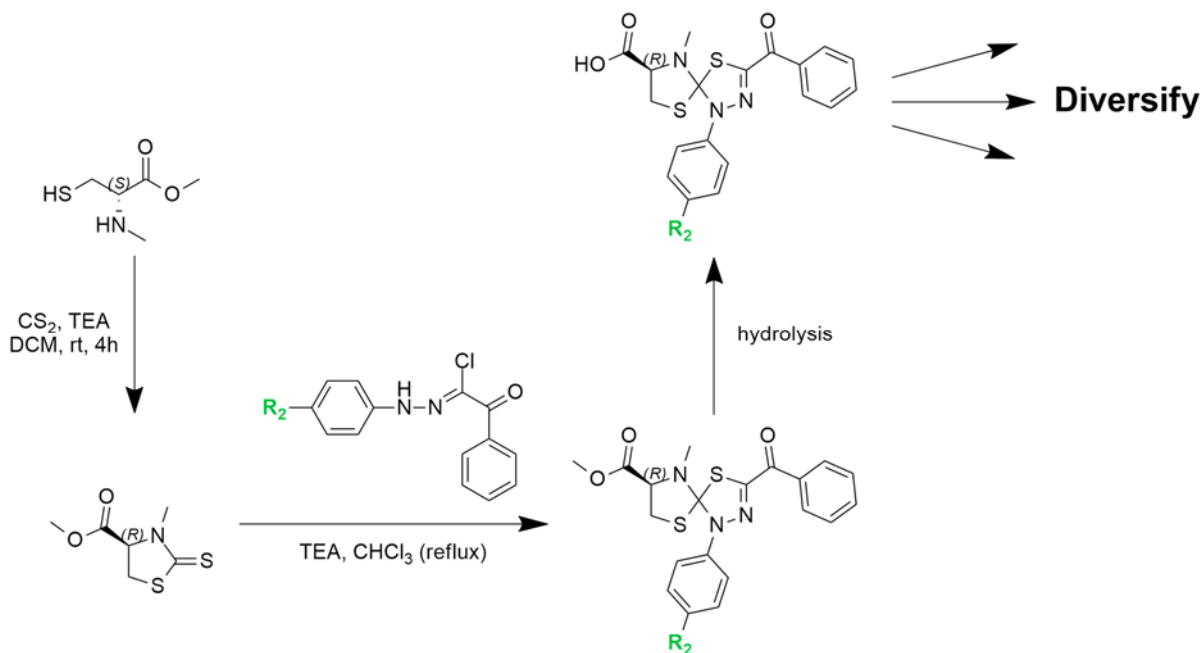
Despite lacking an increase in activity, the fact that **R₃** does not require substitution can save on molecular weight, which can be valuable if **5f** were to be used in cell or animal assays. Changing the **R₃** substitution did not cause a marked change in K_i when **R₂** is *p*-methoxyaniline which suggests that more changes to **R₃** could be made to enhance binding. Nonetheless, any one of these three compounds can be used to study the effects of JHDM1A inhibition and, more specifically, as orthogonal tools to reinforce data gained by another inhibitor with a more common structural motif.

There is still room for improvement, as there were some places where substitution made little-to-no change in binding. Of course, the most obvious improvement to this series would be to obtain enantiopure compounds for bioassay, as the synthesis route is not enantioselective. Because each final mixture is a 1:1 ratio of enantiomers, it's possible that potency can increase by up to 2x if the preferred, enantiopure stereoisomer was prepared.

Moving forward, it would be useful to make a few more comparable substitutions, specifically on **R₁** since no aryl-substitutions were made for this SAR. The aromatic ring is obviously required for desirable activity so substitutions may allow this series to be fine-tuned for optimal binding. Furthermore, a *para*-ethyl substitution on **R₂** would be a great comparator to **5f** to make a final decision as to whether the ethereal oxygen is necessary for binding, as it is apparent that anything larger would not be tolerated in this position.

The rhodanine methylene was explored as a site of variation via aldol condensation reactions, but this moiety could feasibly be varied further by synthesizing rhodanine esters from an *N*-methyl cysteine ester using carbon disulfide and base, followed by a Japp-Klingemann reaction and 1,3-dipolar cyclization to reach the spiro-compound containing a rhodanine methyl ester (**Scheme 2.5**).⁴⁸ From here, the compound could be hydrolyzed to form the carboxylic acid and various coupling reactions could be used to make substitutions, such as amide coupling with HATU or HBTU.⁴⁹ This method creates an

additional stereocenter, but the amino acid methyl ester can be purchased as the pure enantiomer and the stereocenter remains unchanged throughout all steps. This also allows for the synthesis of enantiopure material because the new stereocenter remains unchanged throughout synthesis and diastereomers can be separated by normal flash chromatography.



Scheme 2.5. Rhodanine methyl ester synthesis for diversification.

It is possible that this series could lead to pharmaceutical development. For this to happen, at least two additional preliminary biological assays would be essential before investing time in development. The first is that solubility of these compounds should be evaluated, as I observed these compounds to be soluble only in highly nonpolar solvents, which makes sense when one considers the high cLogP and low total polar surface area. Secondly, an *in-vitro* cell assay should be developed and conducted to be sure there are no anti-targets affected by the compounds.

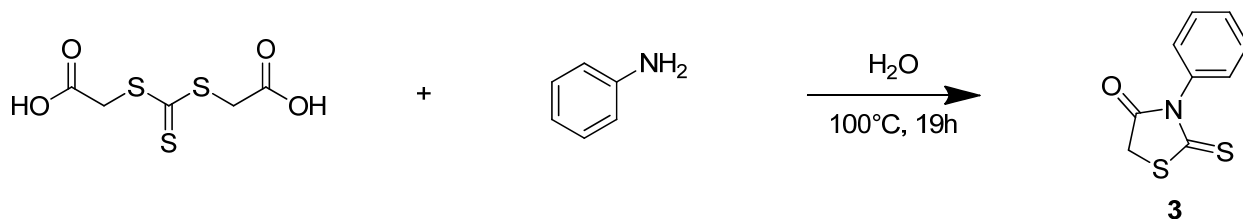
2.6 CONCLUDING REMARKS

The purpose of this study was to tune the binding and reactivity of the previously identified JHDM1A inhibitor, HTS12214. By conducting a structure-activity relationship study, I have synthesized

three analogs (**5f**, **5x**, and **5y**) with 12-to-13-fold increased binding affinity for JHDM1A. This increase in binding affinity appears to be afforded primarily by the presence of *p*-methoxyaniline in the **R₂** position. The fact that changing the **R₃** substitution yielded a negligible increase in binding suggests that the **R₃** position could tolerate additional changes. Additionally, this series can also tolerate changes at the rhodanine methylene position, potentially allowing this compound to be used in development of a wide range of chemical probes.

There is a great need for HDM inhibitors not only for the progress of clinical treatment, but to give the scientific community the tools necessary to understand the intricate workings of this class of enzymes. Currently, many of the histone demethylase inhibitors are modeled after known inhibitors of functionally similar enzymes, which leaves them somewhat lacking in selectivity. To understand the job and function of each type of HDM, greater inhibitor specificity is needed. Although a fair number of HDM crystal structures have been obtained, many of the HDM structures are still unknown (such as JHDM1A). While the series presented herein could potentially be used as an orthogonal tool to verify the validity of bioassay findings, it is essential that we find novel scaffolds with specificity for subsets of HDMs and ultimately compounds that greatly prefer binding to one HDM above all others. It has become obvious that HDMs play a role in various cancers, as methylation state is clearly linked not just to the development and progression of cancer, but to the development of neurological and behavioral issues, as well. Having the ability to control histone methylation patterns would allow the slow-crawl pace of research in this area to become an all-out sprint toward a full understanding of epigenetic regulation, a better understanding of epigenetic mental disorders, and most certainly allow advancement toward more viable long-term oncological treatment options.

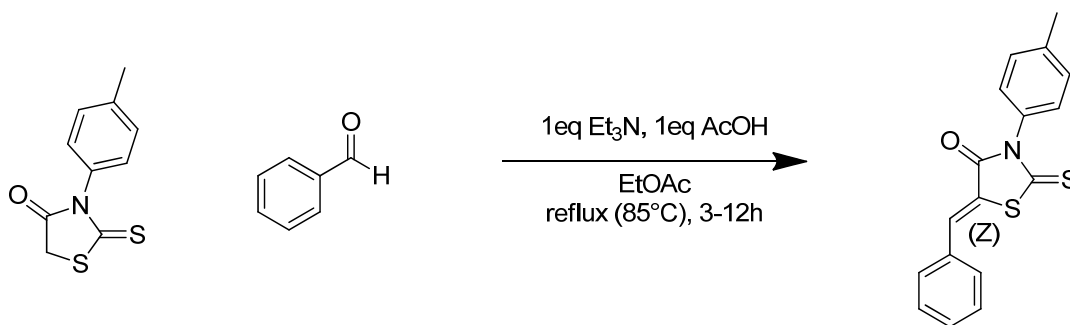
spaced 5 minutes apart. The reaction was stirred at 0 °C for fifteen minutes, when ¹H NMR showed that all *p*-toluidine had been converted to diazo-*p*-toluidine. In a separate flask, **1** (492mg, 2.5mmol, 1 eq.) was dissolved in 12.0mL ethanol to a concentration of 0.2M and cooled to 0 °C while stirring, then sodium acetate (328mg, 4.0mmol, 1.6 eq.) was added. The diazo-*p*-toluidine solution was added directly to this reaction in 4 small aliquots, spaced 5 minutes apart while the temperature of both solutions was maintained at 0 °C (in some cases, the aniline solution was partially neutralized with 0.8eq NaOAc). pH was maintained as close to 5.0 as possible and readjusted after addition of each aliquot. Stirring at 0 °C was continued for thirty minutes longer after addition was completed. Stirring was discontinued and the reaction was then refrigerated overnight. During this time, a precipitate would sometimes form. The referenced procedures stated that this precipitate should be collected by vacuum filtration, but it was observed that the desired product remained in the organic phase and the white solid that remained was sodium acetate. The organic phase was washed with water (2x 15mL) and brine (2x 15mL) before concentrating in vacuo. The resulting film was recrystallized from dichloromethane by addition of hexanes. The solid yellow crystals were collected by vacuum filtration, a 77% yield (497.9mg, 0.647mmol). ¹H NMR (400 MHz, Chloroform-*d*) δ 8.67 (s, 1H), 8.09 – 7.96 (m, 2H), 7.53 – 7.45 (m, 3H), 7.09 (dd, 4H), 2.32 (s, 3H).³⁸



3-phenyl-2-thioxothiazolidin-4-one

In a sealed tube, bis(carboxymethyl)trithiocarbonate (622mg, 2.75mmol, 1.1eq) was dissolved in 5.00mL water (to make a 0.5M solution). The solution was stirred while heating to 95 °C. Aniline (525μL,

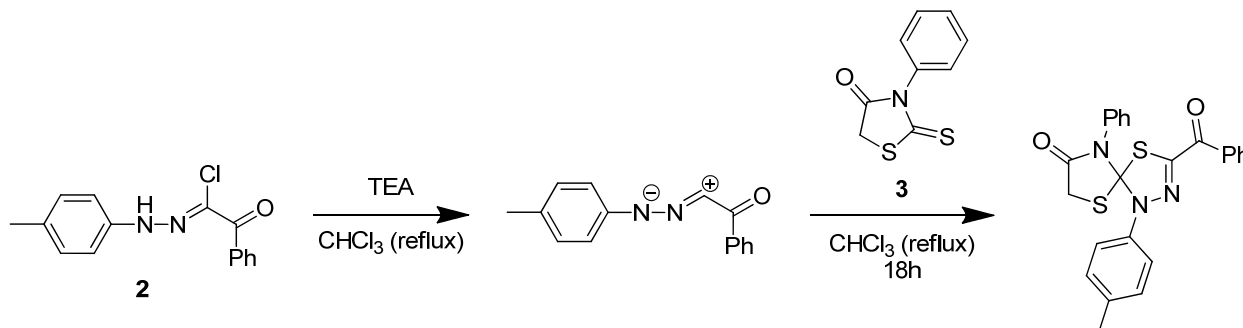
5.00mmol, 1.0eq) was then added before increasing the temperature to reflux. The reaction was stirred overnight, usually a period of 16-19 hours and during this time, the desired product crashed out of solution. The reaction was cooled to room temperature and extracted with ethyl acetate (3x 5mL), washed with water and brine (3x 5mL each), and dried over anhydrous Na_2SO_4 . The resulting solution was then concentrated under reduced pressure and dried for one hour in vacuo leaving a fine, yellow powder in 93.65% yield (490mg, 2.341mmol). ^1H NMR (400 MHz, Chloroform-*d*) δ 7.58 – 7.48 (m, 3H), 7.23 – 7.18 (m, 2H), 4.20 (s, 2H).³⁹



(Z)-5-benzylidene-2-thioxo-3-(p-tolyl)thiazolidin-4-one

In a sealed tube, to a 2.0M solution of 2-thioxo-3-(p-tolyl)thiazolidin-4-one (100mg, 2.50mmol, 1.0eq) in ethyl acetate (1.25mL) was added triethylamine (348 μL , 2.50mmol, 1.0eq) followed by benzaldehyde (542 μL , 2.50mmol, 1.0eq) and finally acetic acid (143 μL , 2.50mmol, 1.0eq). The tube was sealed and the reaction was heated to reflux while stirring for 6 hours. The reaction was then cooled to room temperature and hexanes was added, causing a yellow precipitate to form. The suspension was filtered and washed with hexanes and dried. The resulting crude powder was dissolved in a small amount of dichloromethane and loaded onto silica gel for flash chromatography using hexanes/ethyl acetate (0-30%). Fractions containing pure desired product were combined and concentrated under reduced pressure leaving behind a yellow solid in 51.12% yield (398mg, 1.278mmol). ^1H NMR (500 MHz,

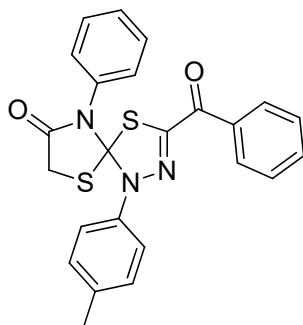
Chloroform-*d* δ 7.82 (s, 1H), 7.60 – 7.48 (m, 6H), 7.38 (d, J = 8.1 Hz, 2H), 7.19 (d, J = 8.3 Hz, 2H), 2.46 (s, 3H).⁴⁷



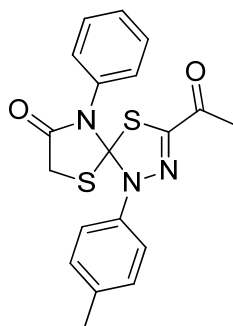
3-benzoyl-9-phenyl-1-(p-tolyl)-4,6-dithia-1,2,9-triazaspiro[4.4]non-2-en-8-one

In a sealed tube, **2** (35mg, 0.168mmol, 1.2eq) and **3** (38mg, 0.140mmol, 1.0eq) were dissolved in 1.1mL chloroform (to make a 0.125M solution) and heated, while stirring, until fully dissolved. Triethylamine (20 μ L, 0.150mmol, 1.1eq) was then added, the tube was sealed and the reaction was heated to reflux while stirring overnight. The reaction was then cooled to room temperature and extracted with ethyl acetate (3x 2mL), washed with water, 1.0N HCl, and brine (3x 2mL each) then dried over anh. Na₂SO₄, filtered and concentrated under reduced pressure. The resulting film was then dissolved in dichloromethane and loaded onto silica gel for flash chromatography using hexanes/ethyl acetate (0-30%). Fractions containing pure desired product were combined and concentrated under reduced pressure, then triturated with methanol and concentrated again to yield a yellow solid in 21.6% yield (13mg, 0.029mmol). For some compounds, purity could be achieved by trituration with diethyl ether or crystallization from dichloromethane or acetone by addition of hexanes. ¹H NMR (400 MHz, Chloroform-*d*) δ 7.94 (d, J = 7.1 Hz, 2H), 7.54 (t, J = 7.4 Hz, 1H), 7.40 (dt, J = 6.4, 3.5 Hz, 5H), 7.34 (d, J = 8.6 Hz, 2H), 7.29 – 7.23 (m, 4H), 3.97 – 3.75 (m, 2H), 2.41 (s, 3H).⁴⁰

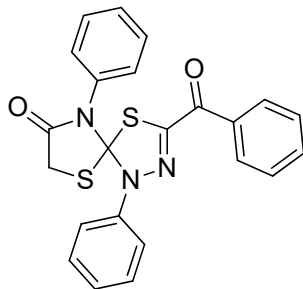
CHAPTER 4 CHARACTERIZATION DATA



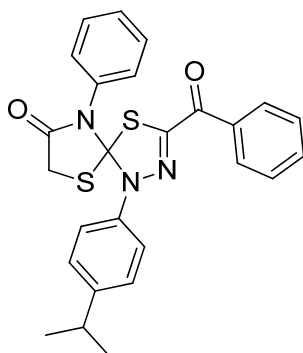
3-benzoyl-9-phenyl-1-(p-tolyl)-4,6-dithia-1,2,9-triazaspiro[4.4]non-2-en-8-one (5a). Yellow solid, 81.8%; ^1H NMR (400 MHz, Chloroform-*d*) δ 7.98 – 7.88 (m, 2H), 7.56 – 7.49 (m, 1H), 7.42 – 7.34 (m, 5H), 7.34 – 7.30 (m, 2H), 7.28 – 7.21 (m, 4H), 3.92 (d, $J = 16.0$ Hz, 1H), 3.77 (d, $J = 16.0$ Hz, 1H), 2.39 (s, 3H).



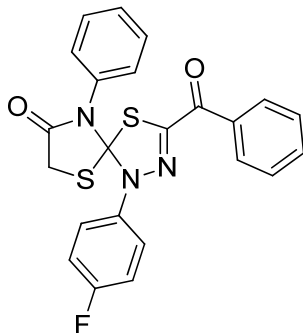
3-acetyl-9-phenyl-1-(p-tolyl)-4,6-dithia-1,2,9-triazaspiro[4.4]non-2-en-8-one (5b). Yellow solid, 3.9%; ^1H NMR (400 MHz, Chloroform-*d*) δ 7.42 – 7.37 (m, 3H), 7.35 – 7.31 (m, 2H), 7.23 (d, $J = 0.8$ Hz, 2H), 7.22 – 7.18 (m, 2H), 3.90 (d, $J = 16.0$ Hz, 1H), 3.72 (d, $J = 16.0$ Hz, 1H), 2.40 (s, 3H), 2.30 (s, 3H).



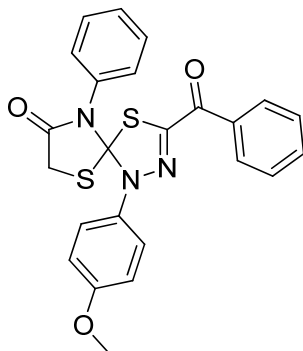
3-benzoyl-1,9-diphenyl-4,6-dithia-1,2,9-triazaspiro[4.4]non-2-en-8-one (5c). Yellow solid, 27.0%; ^1H NMR (500 MHz, Chloroform-*d*) δ 7.95 – 7.91 (m, 2H), 7.57 – 7.52 (m, 1H), 7.48 – 7.36 (m, 9H), 7.32 (tt, $J = 7.1$, 1.9 Hz, 1H), 7.25 – 7.23 (m, 2H), 3.98 (d, $J = 16.1$ Hz, 1H), 3.83 (d, $J = 16.1$ Hz, 1H).



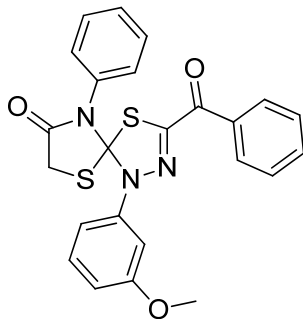
3-benzoyl-1-(4-isopropylphenyl)-9-phenyl-4,6-dithia-1,2,9-triazaspiro[4.4]non-2-en-8-one (5d). Bright yellow solid, 46.1%; ^1H NMR (400 MHz, Chloroform-*d*) δ 7.96 – 7.92 (m, 2H), 7.55 – 7.50 (m, 1H), 7.42 – 7.33 (m, 8H), 7.32 – 7.24 (m, 3H), 3.93 (d, $J = 16.0$ Hz, 1H), 3.78 (d, $J = 16.0$ Hz, 1H), 2.96 (hept, $J = 6.9$ Hz, 1H), 1.29 (d, $J = 6.9$ Hz, 6H); ^{13}C NMR (101 MHz, Chloroform-*d*) δ 183.67, 167.97, 147.23, 143.30, 138.14, 135.08, 134.73, 133.28, 130.10, 129.58, 129.53, 129.43, 128.32, 127.49, 120.90, 104.89, 34.85, 33.71, 29.80, 24.05.



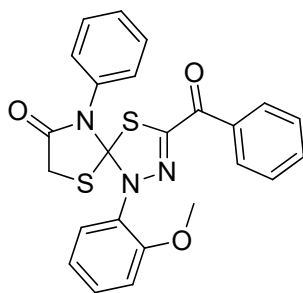
3-benzoyl-1-(4-fluorophenyl)-9-phenyl-4,6-dithia-1,2,9-triazaspiro[4.4]non-2-en-8-one (5e). Yellow solid, 58%; ^1H NMR (400 MHz, Chloroform-*d*) δ 7.94 – 7.89 (m, 2H), 7.58 – 7.52 (m, 1H), 7.45 – 7.37 (m, 7H), 7.27 – 7.22 (m, 2H), 7.19 – 7.12 (m, 2H), 3.95 (d, J = 16.1 Hz, 1H), 3.75 (d, J = 16.1 Hz, 1H).



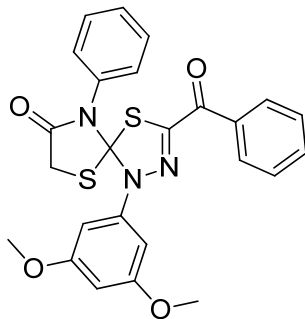
3-benzoyl-1-(4-methoxyphenyl)-9-phenyl-4,6-dithia-1,2,9-triazaspiro[4.4]non-2-en-8-one (5f). Yellow solid, 51.3%; ^1H NMR (400 MHz, Chloroform-*d*) δ 7.99 – 7.93 (m, 2H), 7.57 – 7.51 (m, 1H), 7.46 – 7.34 (m, 7H), 7.33 – 7.27 (m, 2H), 7.00 – 6.95 (m, 2H), 3.91 – 3.83 (m, 4H), 3.67 (d, J = 16.0 Hz, 1H).



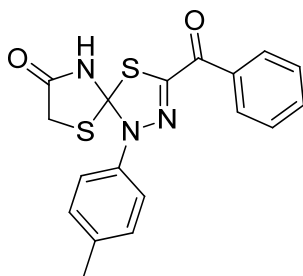
3-benzoyl-1-(3-methoxyphenyl)-9-phenyl-4,6-dithia-1,2,9-triazaspiro[4.4]non-2-en-8-one (5g). Bright yellow solid, 14.0%; $^1\text{H NMR}$ (400 MHz, Chloroform-*d*) δ 7.95 – 7.90 (m, 2H), 7.57 – 7.51 (m, 1H), 7.43 – 7.32 (m, 7H), 7.26 – 7.22 (m, 2H), 7.02 – 6.98 (m, 1H), 6.87 – 6.81 (m, 1H), 3.99 (d, $J = 16.0, 0.6$ Hz, 1H), 3.87 (d, $J = 16.0, 0.6$ Hz, 1H), 3.84 – 3.80 (m, 3H).



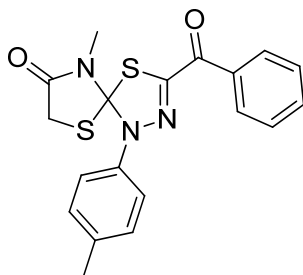
3-benzoyl-1-(2-methoxyphenyl)-9-phenyl-4,6-dithia-1,2,9-triazaspiro[4.4]non-2-en-8-one (5h). Orange solid, 40.8%; $^1\text{H NMR}$ (400 MHz, Chloroform-*d*) δ 7.98 – 7.92 (m, 2H), 7.55 – 7.48 (m, 3H), 7.46 – 7.40 (m, 3H), 7.40 – 7.33 (m, 4H), 7.07 (dd, $J = 8.3, 1.3$ Hz, 1H), 7.00 (ddd, $J = 7.4, 1.3$ Hz, 1H), 3.89 (s, 3H), 3.65 (d, $J = 15.6$ Hz, 1H), 3.36 (d, $J = 15.6$ Hz, 1H).



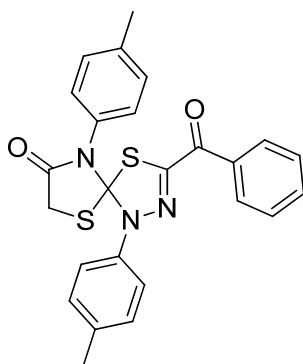
3-benzoyl-1-(3,5-dimethoxyphenyl)-9-phenyl-4,6-dithia-1,2,9-triazaspiro[4.4]non-2-en-8-one (5i). Dark yellow solid, 59.9%; ^1H NMR (400 MHz, Chloroform-*d*) δ 7.95 – 7.91 (m, 2H), 7.57 – 7.51 (m, 1H), 7.43 – 7.35 (m, 6H), 7.26 – 7.23 (m, 1H), 6.60 (d, 2H), 6.39 (t, $J = 2.2$ Hz, 1H), 4.00 (d, $J = 16.0$ Hz, 1H), 3.90 (d, $J = 16.0$ Hz, 1H), 3.79 (s, 6H).



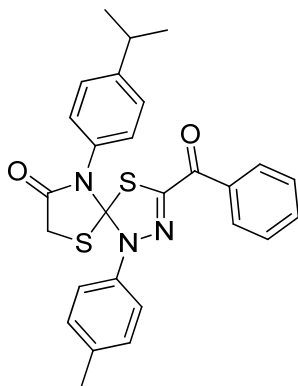
3-benzoyl-1-(p-tolyl)-4,6-dithia-1,2,9-triazaspiro[4.4]non-2-en-8-one (5j). Light orange solid, 15.3%; ^1H NMR (500 MHz, Chloroform-*d*) δ 8.38 – 8.31 (m, 2H), 7.80 – 7.75 (m, 2H), 7.70 – 7.65 (m, 1H), 7.53 (t, 2H), 7.36 (d, 2H), 3.54 (d, $J = 7.9$ Hz, 2H), 2.46 (s, 3H).



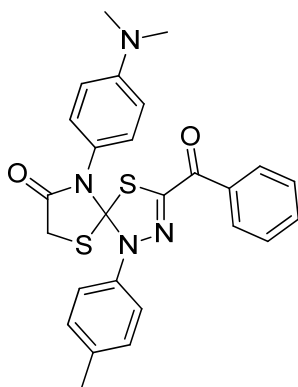
3-benzoyl-9-methyl-1-(p-tolyl)-4,6-dithia-1,2,9-triazaspiro[4.4]non-2-en-8-one (5k). Light yellow solid, 87.3%; ^1H NMR (500 MHz, Chloroform-*d*) δ 8.24 – 8.20 (m, 2H), 7.62 – 7.56 (m, 1H), 7.46 (t, $J = 7.8$ Hz, 2H), 7.18 (s, 4H), 3.71 (d, $J = 15.7$ Hz, 1H), 3.47 (d, 1H), 3.02 (s, 3H), 2.37 (s, 3H).



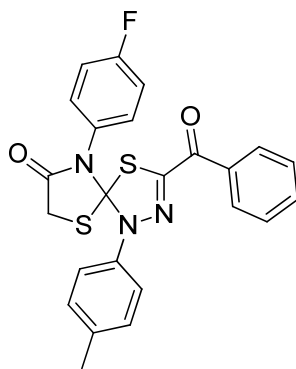
3-benzoyl-1,9-di-p-tolyl-4,6-dithia-1,2,9-triazaspiro[4.4]non-2-en-8-one (5l). Orange solid, 40.35%; ^1H NMR (400 MHz, Chloroform-*d*) δ 7.99 – 7.93 (m, 2H), 7.58 – 7.52 (m, 1H), 7.40 (t, $J = 7.8$ Hz, 2H), 7.35 – 7.30 (m, 2H), 7.26 – 7.17 (m, 4H), 7.13 (d, $J = 8.4$ Hz, 2H), 3.92 (d, $J = 16.0$ Hz, 1H), 3.76 (d, $J = 16.0$ Hz, 1H), 2.40 (s, 3H), 2.31 (s, 3H).



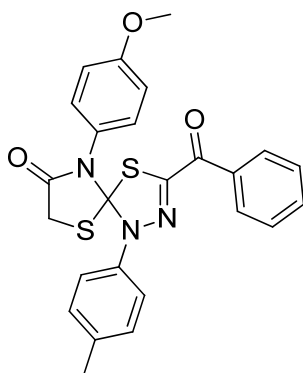
3-benzoyl-9-(4-isopropylphenyl)-1-(p-tolyl)-4,6-dithia-1,2,9-triazaspiro[4.4]non-2-en-8-one (5m). Bright yellow solid, 41.0%; $^1\text{H NMR}$ (400 MHz, Chloroform-*d*) δ 7.90 – 7.87 (m, 2H), 7.56 – 7.50 (m, 1H), 7.41 – 7.35 (m, 2H), 7.33 – 7.29 (m, 2H), 7.26 – 7.22 (m, 4H), 7.19 – 7.15 (m, 2H), 3.93 (d, $J = 15.9$, 0.5 Hz, 1H), 3.77 (d, $J = 15.9$, 0.5 Hz, 1H), 2.86 (hept, $J = 6.9$ Hz, 1H), 2.40 (s, 3H), 1.16 (d, $J = 7.0$, 0.5 Hz, 6H).



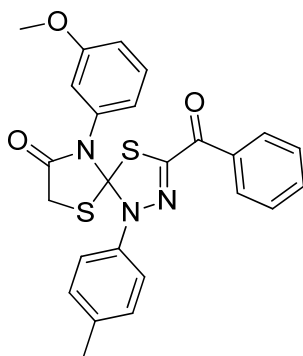
3-benzoyl-9-(4-(dimethylamino)phenyl)-1-(p-tolyl)-4,6-dithia-1,2,9-triazaspiro[4.4]non-2-en-8-one (5n). Yellow solid, 86.4%; $^1\text{H NMR}$ (400 MHz, Chloroform-*d*) δ 7.97 – 7.91 (m, 2H), 7.54 – 7.48 (m, 1H), 7.40 – 7.34 (m, 2H), 7.33 – 7.28 (m, 2H), 7.23 – 7.18 (m, 2H), 7.07 – 7.01 (m, 2H), 6.65 – 6.58 (m, 2H), 3.90 (d, $J = 16.0$ Hz, 1H), 3.76 (d, $J = 15.9$ Hz, 1H), 2.89 (s, 6H), 2.38 (s, 3H).



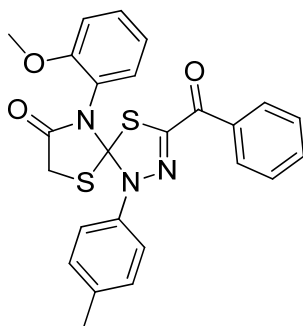
3-benzoyl-9-(4-fluorophenyl)-1-(p-tolyl)-4,6-dithia-1,2,9-triazaspiro[4.4]non-2-en-8-one (5o). Red-orange solid, 8.4%; $^1\text{H NMR}$ (500 MHz, Chloroform-*d*) δ 8.00 – 7.95 (m, 2H), 7.55 (ddt, $J = 8.8, 7.1, 1.3$ Hz, 1H), 7.44 – 7.38 (m, 2H), 7.33 – 7.28 (m, 2H), 7.26 – 7.21 (m, 4H), 7.10 – 7.06 (m, 2H), 3.93 (d, $J = 16.1$ Hz, 1H), 3.78 (d, $J = 16.1$ Hz, 1H), 2.40 (s, 3H).



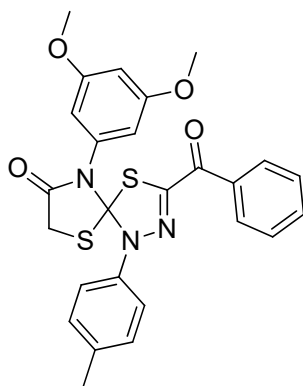
3-benzoyl-9-(4-methoxyphenyl)-1-(p-tolyl)-4,6-dithia-1,2,9-triazaspiro[4.4]non-2-en-8-one (5p). Yellow solid, 9.1%; $^1\text{H NMR}$ (500 MHz, Chloroform-*d*) δ 7.98 – 7.94 (m, 2H), 7.57 – 7.51 (m, 1H), 7.43 – 7.37 (m, 2H), 7.33 – 7.29 (m, 2H), 7.26 – 7.22 (m, 2H), 7.17 – 7.13 (m, 2H), 6.91 – 6.86 (m, 2H), 3.93 (d, $J = 16.0$ Hz, 1H), 3.79 (d, $J = 16.1$ Hz, 1H), 3.75 (s, 3H), 2.40 (s, 3H).



3-benzoyl-9-(3-methoxyphenyl)-1-(p-tolyl)-4,6-dithia-1,2,9-triazaspiro[4.4]non-2-en-8-one (5q). Bright yellow solid, 29.2%; $^1\text{H NMR}$ (400 MHz, Chloroform-*d*) δ 7.97 (ddt, $J = 7.5, 1.6, 1.0$ Hz, 2H), 7.58 – 7.51 (m, 1H), 7.44 – 7.37 (m, 2H), 7.36 – 7.27 (m, 3H), 7.25 – 7.22 (m, 2H), 6.93 – 6.84 (m, 2H), 6.79 (d, $J = 2.3$ Hz, 1H), 3.91 (d, $J = 16.0, 0.8$ Hz, 1H), 3.75 (d, 1H), 3.71 (s, 3H), 2.40 (s, 3H).

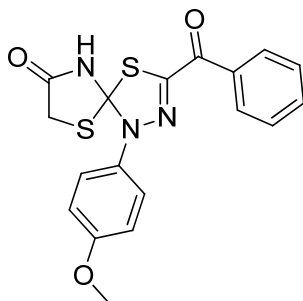


3-benzoyl-9-(2-methoxyphenyl)-1-(p-tolyl)-4,6-dithia-1,2,9-triazaspiro[4.4]non-2-en-8-one (5r). Bright yellow solid, 37.4%; $^1\text{H NMR}$ (400 MHz, Chloroform-*d*) δ 8.03 – 7.98 (m, 2H), 7.57 – 7.51 (m, 1H), 7.44 – 7.33 (m, 6H), 7.28 – 7.23 (m, 1H), 7.14 (dd, $J = 7.8, 1.7$ Hz, 1H), 7.03 (dd, $J = 8.4, 1.3$ Hz, 1H), 6.89 (td, $J = 7.7, 1.3$ Hz, 1H), 3.96 (d, $J = 15.9$ Hz, 1H), 3.90 (s, 3H), 3.73 (d, $J = 15.9$ Hz, 1H), 2.40 (s, 3H).

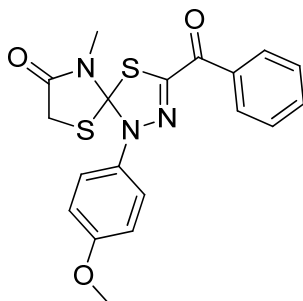


3-benzoyl-9-(3,5-dimethoxyphenyl)-1-(p-tolyl)-4,6-dithia-1,2,9-triazaspiro[4.4]non-2-en-8-one (5s).

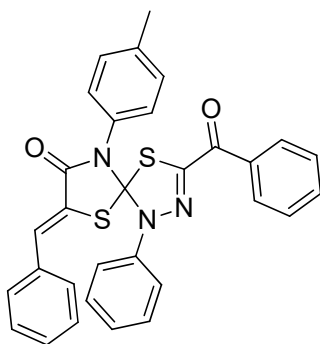
Yellow solid, 59.3%; ^1H NMR (400 MHz, Chloroform-*d*) δ 8.03 – 7.97 (m, 2H), 7.58 – 7.52 (m, 1H), 7.47 – 7.38 (m, 2H), 7.37 – 7.30 (m, 2H), 7.25 – 7.21 (m, 2H), 6.44 (t, 1H), 6.41 (d, $J = 2.2, 0.5$ Hz, 2H), 3.89 (d, $J = 16.0, 0.4$ Hz, 1H), 3.72 (d, $J = 16.0, 0.5$ Hz, 1H), 3.68 (s, 6H), 2.39 (s, 3H); ^{13}C NMR (101 MHz, Chloroform-*d*) δ 183.67, 167.97, 147.23, 143.30, 138.14, 135.08, 134.73, 133.28, 130.10, 129.58, 129.53, 129.43, 128.32, 127.49, 120.90, 104.89, 34.85, 33.71, 29.80, 24.05.



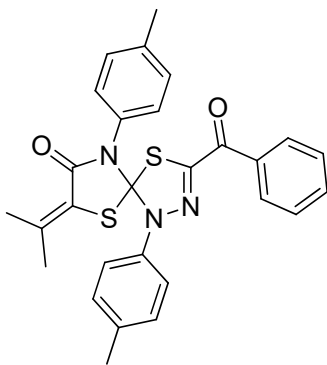
3-benzoyl-1-(4-methoxyphenyl)-4,6-dithia-1,2,9-triazaspiro[4.4]non-2-en-8-one (5t). Orange oil, 3.9%; ^1H NMR (500 MHz, Chloroform-*d*) δ 8.33 – 8.29 (m, 2H), 7.88 – 7.83 (m, 2H), 7.65 (t, $J = 7.4$ Hz, 1H), 7.51 (t, $J = 7.8$ Hz, 3H), 7.06 – 7.01 (m, 2H), 3.87 (s, 3H), 3.83 (s, 2H).



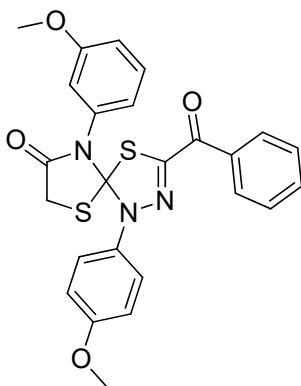
3-benzoyl-1-(4-methoxyphenyl)-9-methyl-4,6-dithia-1,2,9-triazaspiro[4.4]non-2-en-8-one (5u). Dark red-orange oil, 15.2%; ^1H NMR (500 MHz, Chloroform-*d*) δ 8.22 – 8.18 (m, 2H), 7.57 (t, $J = 7.4$ Hz, 1H), 7.45 (t, $J = 7.8$ Hz, 3H), 7.24 – 7.21 (m, 2H), 6.93 – 6.89 (m, 2H), 3.82 (s, 3H), 3.64 (d, $J = 15.7$ Hz, 1H), 3.35 (d, $J = 15.7$ Hz, 1H), 3.04 (s, 3H).



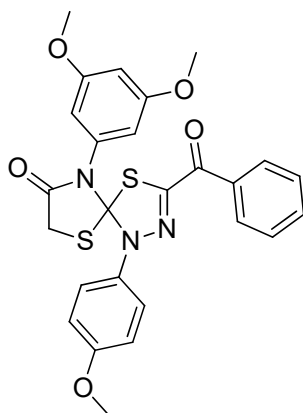
(Z)-3-benzoyl-7-benzylidene-1-phenyl-9-(p-tolyl)-4,6-dithia-1,2,9-triazaspiro[4.4]non-2-en-8-one (5v). Yellow solid, 15.87%; ^1H NMR (500 MHz, Chloroform-*d*) δ 7.96 (d, $J = 7.0$ Hz, 1H), 7.83 (s, 1H), 7.57 (t, $J = 7.4$ Hz, 1H), 7.49 (d, $J = 7.4$ Hz, 3H), 7.46 – 7.41 (m, 4H), 7.41 – 7.31 (m, 4H), 7.22 – 7.15 (m, 4H), 7.09 (d, $J = 8.3$ Hz, 2H), 2.31 (s, 3H).



3-benzoyl-7-(propan-2-ylidene)-1,9-di-p-tolyl-4,6-dithia-1,2,9-triazaspiro[4.4]non-2-en-8-one (5w). Dark yellow solid, 17.2%; $^1\text{H NMR}$ (500 MHz, Chloroform-*d*) δ 7.91 (dd, $J = 8.4, 1.3$ Hz, 2H), 7.57 – 7.52 (m, 1H), 7.40 (t, $J = 7.8$ Hz, 2H), 7.32 – 7.28 (m, 2H), 7.19 (d, $J = 8.4$ Hz, 2H), 7.14 (d, $J = 8.1$ Hz, 2H), 7.07 (d, $J = 8.4$ Hz, 2H), 2.42 (s, 3H), 2.37 (s, 3H), 2.28 (s, 3H), 1.90 (s, 3H).



3-benzoyl-9-(3-methoxyphenyl)-1-(4-methoxyphenyl)-4,6-dithia-1,2,9-triazaspiro[4.4]non-2-en-8-one (5x). Yellow solid, 49.0%; $^1\text{H NMR}$ (400 MHz, Chloroform-*d*) δ 8.00 – 7.95 (m, 2H), 7.57 – 7.49 (m, 1H), 7.43 – 7.34 (m, 4H), 7.29 (t, $J = 8.4, 7.9$ Hz, 1H), 6.97 – 6.92 (m, 2H), 6.91 – 6.86 (m, 2H), 6.82 – 6.80 (m, 1H), 3.86 – 3.80 (m, 4H), 3.71 (d, $J = 0.5$ Hz, 3H), 3.62 (dd, $J = 16.0, 0.5$ Hz, 1H).



3-benzoyl-9-(3,5-dimethoxyphenyl)-1-(4-methoxyphenyl)-4,6-dithia-1,2,9-triazaspiro[4.4]non-2-en-8-one
(5y). Yellow solid, 85.0%; $^1\text{H NMR}$ (400 MHz, Chloroform-*d*) δ 8.02 – 7.97 (m, 2H), 7.57 – 7.49 (m, 1H),
7.42 – 7.35 (m, 4H), 6.97 – 6.91 (m, 2H), 6.43 (s, 3H), 3.83 (s, 3H), 3.80 (d, $J = 16.0$ Hz, 1H), 3.68 (s, 6H),
3.59 (d, $J = 16.0$ Hz, 1H).

REFERENCES

- (1) Zheng, Y.-C.; Ma, J.; Wang, Z.; Li, J.; Jiang, B.; Zhou, W.; Shi, X.; Wang, X.; Zhao, W.; Liu, H.-M. *Med. Res. Rev.* **2015**, *35* (5), 1032–1071.
- (2) Peterson, C. L.; Laniel, M.-A. *Curr. Biol.* **2004**, *14*, R546–R551.
- (3) Marks, P.; Rifkind, R. A.; Richon, V. M.; Breslow, R.; Miller, T.; Kelly, W. K. *Nat. Rev. Cancer* **2001**, *1* (3), 194–202.
- (4) Cloos, P. A. C.; Christensen, J.; Agger, K.; Helin, K. *Genes Dev.* **2008**, *22* (9), 1115–1140.
- (5) Rotili, D.; Mai, A. *Genes Cancer* **2011**, *2* (6), 663–679.
- (6) Greer, E. L.; Shi, Y. *Nat. Rev. Genet.* **2012**, *13* (5), 343–357.
- (7) Shi, X.; Hong, T.; Walter, K. L.; Ewalt, M.; Michishita, E.; Hung, T.; Carney, D.; Peña, P.; Lan, F.; Kaadige, M. R.; Lacoste, N.; Cayrou, C.; Davrazou, F.; Saha, A.; Cairns, B. R.; Ayer, D. E.; Kutateladze, T. G.; Shi, Y.; Cote, J.; Chua, K. F.; Gozani, O. *Nature* **2006**, *442* (7098), 96–99.
- (8) Bernstein, B. E.; Mikkelsen, T. S.; Xie, X.; Kamal, M.; Huebert, D. J.; Cuff, J.; Fry, B.; Meissner, A.; Wernig, M.; Plath, K.; Jaenisch, R.; Wagschal, A.; Feil, R.; Schreiber, S. L.; Lander, E. S. *Cell* **2006**, *125* (2), 315–326.
- (9) Kashyap, V.; Ahmad, S.; Nilsson, E. M.; Helczynski, L.; Kenna, S.; Persson, J. L.; Gudas, L. J.; Mongan, N. P. *Mol. Oncol.* **2013**, *7* (3), 555–566.
- (10) Nakamura, S.; Tan, L.; Nagata, Y.; Takemura, T.; Asahina, A.; Yokota, D.; Yagyu, T.; Shibata, K.; Fujisawa, S.; Ohnishi, K. *Mol. Carcinog.* **2013**, *52* (1), 57–69.
- (11) Wang, Z.; Wang, C.; Huang, X.; Shen, Y.; Shen, J.; Ying, K. *Biochim. Biophys. Acta - Proteins Proteomics* **2012**, *1824* (4), 692–700.
- (12) Shen, Y.; Guo, X.; Wang, Y.; Qiu, W.; Chang, Y.; Zhang, A.; Duan, X. *BMC Cancer* **2012**, *12* (1), 470.
- (13) Elsheikh, S. E.; Green, A. R.; Rakha, E. A.; Powe, D. G.; Ahmed, R. A.; Collins, H. M.; Soria, D.; Garibaldi, J. M.; Paish, C. E.; Ammar, A. A.; Grainge, M. J.; Ball, G. R.; Abdelghany, M. K.; Martinez-Pomares, L.; Heery, D. M.; Ellis, I. O. *Cancer Res.* **2009**, *69* (9), 3802–3809.
- (14) Klose, R. J.; Zhang, Y. *Nat. Rev. Mol. Cell Biol.* **2007**, *8* (4), 307–318.
- (15) Shi, Y. G.; Tsukada, Y. *Cold Spring Harb. Perspect. Biol.* **2013**, *5* (9), 2–4.
- (16) Chen, Z.; Zang, J.; Whetstine, J.; Hong, X.; Davrazou, F.; Kutateladze, T. G.; Simpson, M.; Mao, Q.; Pan, C. H.; Dai, S.; Hagman, J.; Hansen, K.; Shi, Y.; Zhang, G. *Cell* **2006**, *125* (4), 691–702.
- (17) Tsukada, Y.; Fang, J.; Erdjument-Bromage, H.; Warren, M. E.; Borchers, C. H.; Tempst, P.; Zhang, Y. *Nature*. 2006, pp 811–816.
- (18) Cheng, Z.; Cheung, P.; Kuo, A. J.; Yukl, E. T.; Wilmot, C. M.; Gozani, O.; Patel, D. J. *Genes Dev.* **2014**, *28* (16), 1758–1771.
- (19) Klose, R. J.; Kallin, E. M.; Zhang, Y. *Nat. Rev. Genet.* **2006**, *7* (9), 715–727.

- (20) Yamane, K.; Toumazou, C.; Tsukada, Y. ichi; Erdjument-Bromage, H.; Tempst, P.; Wong, J.; Zhang, Y. *Cell* **2006**, *125* (3), 483–495.
- (21) Klose, R. J.; Yamane, K.; Bae, Y.; Zhang, D.; Erdjument-Bromage, H.; Tempst, P.; Wong, J.; Zhang, Y. *Nature* **2006**, *442* (7100), 312–316.
- (22) McDonough, M. A.; Loenarz, C.; Chowdhury, R.; Clifton, I. J.; Schofield, C. J. *Curr. Opin. Struct. Biol.* **2010**, *20* (6), 659–672.
- (23) Adamo, A.; Barrero, M. J.; Belmonte, J. C. I. *Cell Cycle* **2011**, *10* (19), 3215–3216.
- (24) Whyte, W. A.; Bilodeau, S.; Orlando, D. A.; Hoke, H. A.; Frampton, G. M.; Foster, C. T.; Cowley, S. M.; Young, R. A. *Nature* **2012**, *482* (7384), 221–225.
- (25) Saleque, S.; Kim, J.; Rooke, H. M.; Orkin, S. H. *Mol. Cell* **2007**, *27* (4), 562–572.
- (26) Mohammad, H. P.; Smitheman, K. N.; Kamat, C. D.; Soong, D.; Federowicz, K. E.; VanAller, G. S.; Schneck, J. L.; Carson, J. D.; Liu, Y.; Butticello, M.; Bonnette, W. G.; Gorman, S. A.; Degenhardt, Y.; Bai, Y.; McCabe, M. T.; Pappalardi, M. B.; Kaspavec, J.; Tian, X.; McNulty, K. C.; Rouse, M.; McDevitt, P.; Ho, T.; Crouthamel, M.; Hart, T. K.; Concha, N. O.; McHugh, C. F.; Miller, W. H.; Dhanak, D.; Tummino, P. J.; Carpenter, C. L.; Johnson, N. W.; Hann, C. L.; Kruger, R. G. *Cancer Cell* **2015**, *28* (1), 57–69.
- (27) Fiedorowicz, J. G.; Swartz, K. L. *J. Psychiatr. Pract.* **2004**, *10* (4), 239–248.
- (28) Yamada, M.; Yasuhara, H. *Neurotoxicology* **2004**, *25* (1–2), 215–221.
- (29) McAllister, T. E.; England, K. S.; Hopkinson, R. J.; Brennan, P. E.; Kawamura, A.; Schofield, C. J. *J. Med. Chem.* **2016**, *59* (4), 1308–1329.
- (30) Morera, L.; Lübbert, M.; Jung, M. *Clin. Epigenetics* **2016**, *8*, 57.
- (31) Kruidenier, L.; Chung, C.; Cheng, Z.; Liddle, J.; Che, K.; Joberty, G.; Bantscheff, M.; Bountra, C.; Bridges, A.; Diallo, H.; Eberhard, D.; Hutchinson, S.; Jones, E.; Katso, R.; Leveridge, M.; Mander, P. K.; Mosley, J.; Ramirez-Molina, C.; Rowland, P.; Schofield, C. J.; Sheppard, R. J.; Smith, J. E.; Swales, C.; Tanner, R.; Thomas, P.; Tumber, A.; Drewes, G.; Oppermann, U.; Patel, D. J.; Lee, K.; Wilson, D. M. *Nature* **2012**, *488* (7411), 404–408.
- (32) King, O. N. F.; Li, X. S.; Sakurai, M.; Kawamura, A.; Rose, N. R.; Ng, S. S.; Quinn, A. M.; Rai, G.; Mott, B. T.; Beswick, P.; Klose, R. J.; Oppermann, U.; Jadhav, A.; Heightman, T. D.; Maloney, D. J.; Schofield, C. J.; Simeonov, A. *PLoS One* **2010**, *5* (11).
- (33) Luo, X.; Liu, Y.; Kubicek, S.; Myllyharju, J.; Tumber, A.; Ng, S.; Che, K. H.; Podoll, J.; Heightman, T. D.; Oppermann, U.; Schreiber, S. L.; Wang, X. *J. Am. Chem. Soc.* **2011**, *133* (24), 9451–9456.
- (34) Xu, W.; Podoll, J. D.; Dong, X.; Tumber, A.; Oppermann, U.; Wang, X. *J Med Chem* **2013**, *56*, 5198–5202.
- (35) Marholz, L. J.; Chang, L.; Old, W. M.; Wang, X. *ACS Chem. Biol.* **2015**, *10* (1), 129–137.
- (36) Wang, W.; Marholz, L. J.; Wang, X. *J. Biomol. Screen.* **2015**, *20* (6), 821–827.
- (37) Chassaing, S.; Isorez-Mahler, G.; Kueny-Stotz, M.; Brouillard, R. *Tetrahedron* **2015**, *71* (20), 3066–3078.

- (38) Shawali, A. S.; Abdelhamid, A. O.; Hassaneen, H. M.; Shetta, A. J. *Heterocycl. Chem.* **1982**, *19* (1), 73–75.
- (39) He, X. Y.; Zou, P.; Qiu, J.; Hou, L.; Jiang, S.; Liu, S.; Xie, L. *Bioorganic Med. Chem.* **2011**, *19* (22), 6726–6734.
- (40) Hassaneen, H. M.; Abunada, N. M.; Miqdad, O. A.; Fares, A. A. *Asian J. Chem.* **2012**, *24* (1), 330–334.
- (41) Kürti, L.; Czakó, B. *Strategic Applications of Named Reactions in Organic Synthesis: Background and Detailed Mechanisms*; Elsevier Academic Press: Amsterdam, 2005.
- (42) Heath-Brown, B.; Philpott, P. G. *J. Chem. Soc.* **1965**, 7185–7193.
- (43) Yao, H. C.; Resnick, P. *J. Am. Chem. Soc.* **1962**, *84* (18), 3514–3517.
- (44) Evans, D. A.; Song, H.-J.; Fandrick, K. R. *Org. Lett.* **2006**, *8* (15), 3351–3354.
- (45) Mlostoń, G.; Urbaniak, K.; Utecht, G.; Lentz, D.; Jasiński, M. *J. Fluor. Chem.* **2016**, *192*, 147–154.
- (46) Böhm, H.-J.; Banner, D.; Bendels, S.; Kansy, M.; Kuhn, B.; Müller, K.; Obst-Sander, U.; Stahl, M. *Chembiochem* **2004**, *5* (5), 637–643.
- (47) Russell, A. J.; Westwood, I. M.; Crawford, M. H. J.; Robinson, J.; Kawamura, A.; Redfield, C.; Laurieri, N.; Lowe, E. D.; Davies, S. G.; Sim, E. *Bioorganic Med. Chem.* **2009**, *17* (2), 905–918.
- (48) Chen, N.; Jia, W.; Xu, J. *European J. Org. Chem.* **2009**, No. 33, 5841–5846.
- (49) Carpino, L. *J. Am. Chem. Soc.* **1993**, *115* (13), 4397–4398.